1988

In situ oligodeoxyribonucleotide probing of a conserved region on the 3' end of Escherichia coli 16S ribosomal RNA

Matthew Amadeo Firpo
The University of Montana

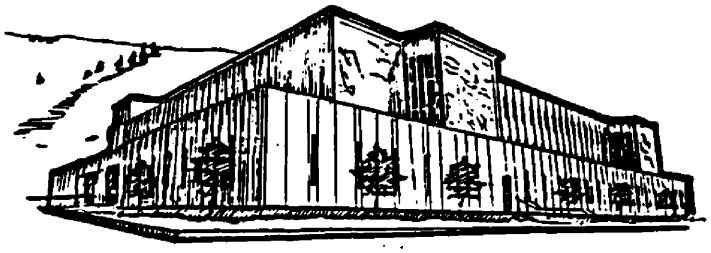

In situ OLIGODEOXYRIBONUCLEOTIDE PROBING OF A CONSERVED REGION ON THE 3' END OF *Escherichia coli* 16S RIBOSOMAL RNA

By

Matthew Amadeo Firpo

B.A., University of Montana, 1984

Presented in partial fulfillment of the requirements

for the degree of

Master of Science

University of Montana

1988

Approved by

Walter E. Hill

Chairman, Board of Examiners

Dean, Graduate School

7-17-92

Date

ProQuest LLC.
789 East Eisenhower Parkway
P.O. Box 1346
Ann Arbor, MI 48106 - 1346

Firpo, Matthew A., M.S., October 1988 Biochemistry

In situ Oligodeoxyribonucleotide Probing of a Conserved Region on the 3' End of *Escherichia coli* 16S Ribosomal RNA (71 pp.)

Director: Walter E. Hill

The structure and function of an evolutionarily conserved region of *E. coli* 16S ribosomal RNA (rRNA) was investigated using complementary oligodeoxyribonucleotide hybridization. The oligonucleotide probes 5'-dACCTTGTTACGACTT (designated 1492-1506) and 5'-dACCTTGTTA (designated 1498-1506) were hybridized to bases 1492-1506 of 16S rRNA in salt-washed 30S ribosomal subunits. The differential accessibility of probes under various conditions was used to draw conclusions about the region's involvement during translational initiation and decoding.

Both probes bound specifically to their target sites suggesting that the region is exposed on 30S subunits. Probe binding was decreased by addition of IF-3 or poly uridylic acid (poly U), but was not further decreased by poly U directed $tRNA^{Phe}$ binding. Activation of subunits decreased probe binding, but to a lesser extent than when IF-3 or poly U was present. The data suggest an intimate involvement of the region during translational initiation and may support the pairing of bases 1394-1395 to bases 1505-1506 upon subunit activation. A model for the decoding site is presented that incorporates these data and other available information.

Preface

I would like to thank the members of my family and my lab for their support throughout this endeavor and throughout the years. I would especially like to thank my mentor, Dr. Walter E. Hill and my friend, Dr. William E. Tapprich. Bill, as soon as you get that gel running, lets go out to Rock Creek for the evening hatch.

This work is dedicated in memory of George Anthony Firpo and Joseph Amadeo Firpo. Plus ça change, plus c'est la même chose. Omnia mutantur, nos et mutamur in illus.

Table of Contents

	page
Abstract	ii
Preface	iii
Table of Contents	iv
List of Tables	v
List of Illustrations	vi
Chapter 1 Introduction	1
Chapter 2 Methods	16
Chapter 3 Results	32
Chapter 4 Discussion	51
References	67

List of Tables

		page
Table I	N° Solutions for Reverse Transcriptase Sequence Analysis.	26
Table II	16S rRNA/Probe Homology Regions	40

List of Illustrations

	page
Figure 1 The Coaxial Stacking Model	11
Figure 2 Probe Target Sites	19
Figure 3 HPLC Profiles of Oligonucleotide Work-up	20
Figure 4 Autoradiogram of ^{32}P Labeled Oligomers	23
Figure 5 Probe 1498-1506 Gradient Binding Assay	33
Figure 6 Probe 1498-1506 Filter Binding Assay	34
Figure 7 Probe 1492-1506 Rnase H Time Titration	35
Figure 8 Probe 1498-1506 RNase H Assay	36
Figure 9 Probe 1498-1506 RNase H Fragment Sequence Analysis	37
Figure 10 Probe 1492-1506 RNase H Assay	38
Figure 11 Active/Inactive Filter Binding Assays	42
Figure 12 Active/Inactive Filter Binding Assays Co-incubated with Probe	43
Figure 13 Probe 1498-1506/Poly U Filter Binding Assays	44
Figure 14 IF-3 Sucrose Density Gradient Binding Assay	46
Figure 15 Probe 1498-1506/IF-3 Competition Assay	47
Figure 16 Probe 1498-1506/IF-3 Filter Binding Assay	48
Figure 17 Subunit Association Assays	49
Figure 18 Probe 787-795/IF-3 Competition Assay	50
Figure 19 Proposed Model for Interactions at the 1500 Region	60

Chapter 1

INTRODUCTION

On the level of the cell, life can be simplified to the relationship of nucleic acids and proteins as represented by the central dogma of molecular biology. The elegant mechanism of nucleotide base pairing allows nucleic acids to store, retrieve and transfer the genetic information. The ultimate goal of this scheme is the production of proteins.

An interesting paradox arises in light of the fact that proteins are intimately involved in every step of this scheme. Protein enzymes are needed to unwind the genomic DNA so that messenger RNA, transfer RNA and ribosomal RNA can be transcribed by other enzymes. Still more proteins are required to translate the genomic message into proteins on the ribosome. Since almost all chemical reactions in a cell are mediated by protein enzymes, it is no wonder that early investigators of the ribosome, itself a ribonucleoprotein complex, thought that the ribosomal proteins were responsible for the chemical reactions involved in joining amino acids to form proteins.

In recent years, evidence has mounted for the participation of RNA in different types of catalytic events. RNA can act as an enzyme singularly as in the self-splicing reactions of Tetrahymena mitochondrial rRNA (Cech, 1987), or with protein co-factors as in reactions involving RNase P (Stark et al., 1978) or small nuclear ribonucleoprotein (snRNP)

complexes (Sharp, 1987). In the more complex case of the ribosome, there is a large body of data suggesting that rRNA acts directly in many events of protein synthesis (Dahlberg, 1989). Such an activity for rRNA should perhaps not be suprising since tRNA and mRNA must bind to the ribosome. It seems logical that the transient binding of these factors be stabilized by base pairing to rRNA. In fact, the first evidence for direct participation of rRNA in protein synthesis came from studies of mRNA binding to ribosomes in E. coli 33where a six base region upsteam of the start codon of all E. coli messenger RNA molecules directly base pairs with a conserved, complementary region of rRNA (Shine and Dalgarno, 1974).

From an evolutionary view, the ability of RNA to act as a catalyst raises the question of which came first, proteins or RNA. The ability of rRNA to process itself in Tetrahymena mitochondria and the participation of rRNA in protein biosynthesis supports the idea that at one time synthesis of proteins may have been carried out by ribosomal RNA alone. Investigation of ribosome structure and function may provide insight into the protein/RNA paradox and the evolutionary beginings of life.

Although the basic scheme of protein biosynthesis is known, relatively little is known about the enzymatic reactions of the ribosome. It is ironic that so much is known about a myriad of protein catalyzed enzymatic reactions and so

little is known about the enzymatic reactions of protein synthesis. Some of the most complex multisubunit protein enzyme systems are understood to such an extent that movement of individual electrons can be traced. Yet, in protein biosynthesis, even basic considerations about substrate binding remain unclear.

Such an inconsistancy may be forgiven in light of the complex nature of the ribosome. Ribosomes can be seen by electron microscopy on rough endoplasmic reticulum of eukaryotes and in the cytoplasm of both eukaryotes and prokaryotes (Spirin, 1986). Electron microscopic studies of the ribosome have resulted in three dimensional models of the ribosomal particle (Lake and Kahan, 1975; Stöffler and Stöffler-Meilicke, 1981; Boublik et al., 1986; Vasiliev et al., 1986). Prokaryotic ribosomes sediment as 70S particles (Hill et al., 1969). Under low salt conditions, this particle can be dissociated into 50S and 30S subunits (Hill et al., 1969). The 50S subunit consists of two strands of RNA (23S rRNA-2904 nucleotides and 5S rRNA-120 nucleotides) and 34 proteins varying in size from 5 to 25 kdal. The 30S subunit is comprised of a 16S RNA moiety (1542 nucleotides) and 21 proteins (8-65 kdal) (Spirin, 1986). In addition to these components, several protein factors that transiently bind the ribosome have been identified. Eukaryotic ribosomes are more complex and studying prokaryotic ribosomes may provide a simple system that can be extrapolated to eukaryotes.

The 30S Ribosomal Subunit

The most extensively characterized ribosomal particle has been the 30S subunit of Escherichia coli. The 30S subunit has a molecular weight of approximately 1 x 10^6 daltons (Van Holde and Hill, 1974). Small-angle X-ray scattering studies suggest that the subunit is best described by an ellipsoid model of dimensions 55 Å x 220 Å x 220 Å (Hill et al., 1969). Models generated from electron microscopic studies indicate the 30S subunit is more asymmetric and prolate with three distinct regions. The elongated body comprises about two-thirds of the subunit and the head about one-third. The two regions are separated by a constriction (Lake and Kahan, 1975; Lake, 1980; Stöffler and Stöffler-Meilicke, 1980; Stöffler and Stöffler-Meilicke, 1986; Boublik et al., 1986; Vasiliev et al., 1986). The third region has been described differently by different investigators. In one model this region is represented as an elongated shelf on one side of the subunit where the body meets the neck (Stöffler and Stöffler-Meilicke, 1980) and in another model, as a platform that extends from the lower two-thirds of the subunit and forms a cleft between itself and the head (Lake, 1980). As described below, the cleft is an important structural feature of the ribosome.

The 30S subunit is approximately two-thirds RNA and one-third protein. The various components can be isolated and then reconstituted to form a functional particle. Studies of the interdependence of ribosomal proteins as they recombine

with the rRNA have lead to an assembly map for the 30S subunit (Nomura and Held, 1974). Protein neighborhoods suggested by this technique are in good agreement with those determined using other approaches (Wittmann, 1983; Moore et al., 1986).

A large body of information has been generated on the placement of ribosomal proteins (r-proteins) relative to themselves and to the EM models (see Giri et al., 1984; Wittmann, 1986 for reviews). Moore and co-workers have recently completed a three-dimensional map of the location of all 21 small subunit proteins, giving distances between protein mass centers of gravity from neutron scattering data (Moore et al., 1986; Capel et al., 1987). This map agrees well with the protein neighborhoods predicted from the assembly map. Other techniques such as singlet-singlet energy transfer (Hardesty et al., 1986; Cantor and Huang, 1975) and protein cross-linking (Traut et al., 1980), although more limited in application, provide further verification of the neutron scattering map.

Superpositioning this three-dimensional protein map onto the electron-microscopic subunit models is facilitated by comparisons with immune electron microscopy (IEM) data. IEM has proven very powerful in topographically placing the r-proteins on the surface of the ribosomal particles by viewing r-protein specific antibody binding using the electron microscope, although the resolution is quite low (Oakes et al., 1986; Stöffler and Stöffler-Meilicke, 1986). Such

placements agree well with the scattering map. The consensus between scattering, IEM and assembly mapping data allows for construction of a reliable three-dimensional model of the small subunit proteins.

16S rRNA

In comparison with the information about small subunit proteins, much less is known about the spatial arrangement of 16S rRNA. As information is generated concerning the role of rRNA in ribosomal activity, more research is directed at delineating functional sites and spatial configurations of rRNA (reviwed in Noller, 1984).

The primary structures of the rRNA components have been determined by sequencing the corresponding rRNA genes (Carbon et al., 1979; Noller, 1980). E. coli 16S rRNA is 1542 nucleotides in length and has 9 methylated bases, most of which are located near the 3′ end (Noller et al., 1986).

Three secondary structure maps for E. coli 16S rRNA have been generated using comparative sequence analysis (Moazed et al., 1986; Brimacombe and Steige, 1985). These structures have been refined and verified to almost complete concensus by various techniques including use of single-and double-strand specific chemical modification reagents and nucleases, thermodynamic stability calculations, RNA cross-linking and nuclear magnetic resonance spectroscopy (see Noller, 1984 and Brimacombe et al., 1986 for reviews).

The tertiary folding of ribosomal RNAs, however, has

proven to be more elusive. A significant undertaking that involves intra-RNA cross-linking between RNA regions distantly located in the primary and secondary structure promises to yield proximal RNA regions in situ (Brimacombe et al., 1986). Mild nuclease digestion studies followed by non-denaturing gel electrophoresis has also proven successful in providing information on tertiary interaction sites (Spitnik-Elson and Elson, 1985).

Another cross-linking technique has been useful in placing r-proteins relative to rRNA (Brimacombe and Steige, 1985). By using bifunctional reagents that cross-link specific amino acid residues with RNA, this technique has the unique ability to locate specific orientations of r-proteins relative to rRNA. Information from this approach agrees well with data from nuclease protection and chemical modification studies where protein binding sites have been located due to their ability to protect certain regions of 16S rRNA (Zimmermann, 1980; Brimacombe et al., 1986; Stern et al., 1989).

Some information about the spatial arrangement of 16S rRNA relative to the 30S subunit has been obtained from immune electron microscopy experiments. Antibodies raised against naturally occurring modified nucleotides and haptenated nucleotides have located several regions of 16S rRNA on the EM model (Stöffler and Stöffler-Meilicke, 1984; Brimacombe and Steige, 1985). Another approach that uses haptens bound to

oligonucleotides that can hybridize with single stranded regions of rRNA has located still more regions (Oakes et al., 1986).

Together, the above techniques give an approximation of the spatial arrangement of 16S rRNA. Combining information on the spatial orientation of the 30S particle with the known functions of certain sites has allowed the definition of discrete functional domains on the ribosome (reviewed in Wittmann, 1986). Futhermore, two models of the tertiary folding of 16S rRNA have recently been presented. One is based mostly on cross-linking data (Brimacombe et al., 1988) and the other, a partial model, is based mostly on chemical modification data (Stern et al., 1988). However, both models combine much of the information known about the spatial arrangements of the 30S components. Although consensus between the two is not complete, refinements to these models as more information becomes available will lead to a complete structure for the 30S subunit.

The Decoding Site

Studies of the secondary structure of E. coli 16S rRNA reveal that approximately 50% of the RNA is involved in base pairing. The major structural result of such base pairing is that regions of RNA fold back on themselves to form double stranded stems with single stranded loops at one end. Many of these loops are present in the secondary structure model and are joined by single stranded regions of RNA.

Comparisons of small subunit RNAs from a multitude of prokaryotes as well as eukaryotic chloroplasts and mitochondria show that, although the sequences vary, the major structural features are retained (Dams et al., 1988). Furthermore, several single stranded regions, both on the loops and in the regions joining stem-loops, are evolutionarily conserved to a considerable extent (Gutell et al., 1985). Such conservation suggests that these regions are required to maintain the functionality of the ribosome, either by helping to maintain a specific conformation or by direct participation in the enzymatic activities of protein biosynthesis.

Six regions of highly-conserved sequence are located throughout 16S rRNA. Two single stranded conserved regions, bases 1394-1408 and 1492-1506, are separated by a stem-loop (the penultimate loop), itself a site of variability between different species. Another single stranded conserved region is located past the ultimate loop between bases 1534 and 1539 (the Shine-Dalgarno region).

Evidence from various experiments suggest that these conserved regions provide the domain where mRNA codons are recognized by the anticodons of tRNA (Noller et al., 1986) and, therefore, the region has been termed the decoding site (Prince et al., 1982). The most convincing support for this argument is the UV-induced cross-linking of base C1400 to the 5′ base of tRNA anticodons (the wobble base). This cross-link

has been induced in high yield in several different systems, both prokaryotic and eukayotic (Schwartz and Ofengand, 1978; Prince et al., 1982; Ofengand et al., 1982). Conditions in which the cross-link occur indicate the tRNA is in the peptidyl-site (P-site), the cross-link is message dependent and the cross-linked tRNA can participate in peptide bond formation (Ofengand et al., 1979).

The idea that the codon-anticodon interaction takes place at the decoding site is further supported by studies of two antibiotics. Resistance to the antibiotic paromomycin is induced by mutations that prevent base-pairing of residues 1409 and 1491 (Noller et al., 1986). Paromomycin induces misreading which suggests a proximity to the site of codon-anticodon interaction. Furthermore,cleavage between residues 1492 and 1493 by colicin E3 results in loss of tRNA binding activity entirely (Noller et al., 1986).

Placement of the decoding site on the 30S model has been facilitated by IEM studies. Two groups have placed the 3′ end of 16S rRNA on the platform side of the cleft (Stöffler and Stöffler-Meilicke, 1986; Oakes et al., 1986) and the methylated adenines on the end of the ultimate loop have been located on the head side of the cleft (Stöffler and Stöffler-Meilicke, 1986). Using an oligomer probe complementary to bases 1392-1408, Lake and co-workers have localized the 1400 conserved region in the cleft as well (Oakes et al., 1986). Confirming the proximity of codon-anticodon interaction to the

conserved regions of the decoding site, mRNA and tRNA have also been mapped in the cleft by IEM (Keren-Zur et al., 1979).

The above, data combined with recent chemical modification studies, have lead Noller and co-workers to propose the induced coaxial stacking model for codon-anticodon pairing in the decoding site (Noller et al., 1986). Chemical modification in the absence and presence of tRNA shows differential modification of bases in the 1400 conserved region (Moazed and Noller, 1986). Protection of bases in this region were seen with intact tRNA bound and when a tRNA anticodon fragment was bound alone suggesting that the protection is due to the anticodon loop of tRNA. Modification of bases C1399, C1400 and G1401 was shown to be message-independent whereas modification of base A1408 on the 1400 conserved side and bases A1492 and A1493 of the 1500 conserved region was only seen when tRNA binding was poly U directed. The coaxial stacking model incorporates these

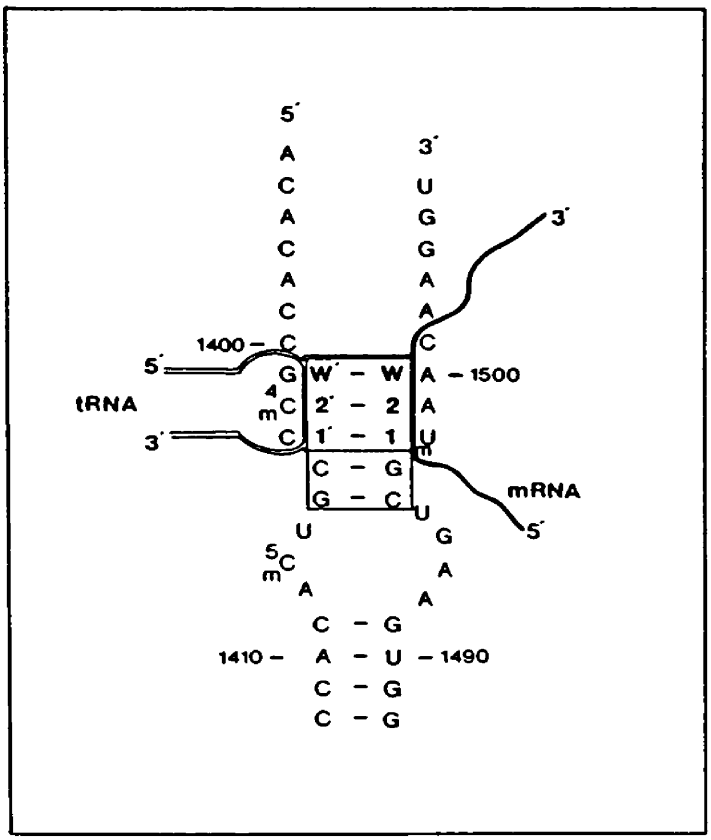

Figure 1 The Coaxial Stacking Model. The codon bases are indicated as 1, 2 and W (wobble base) and the anti-codon bases 1', 2' and W'. This interaction is proposed to stack with the potential base-pairs at 1404-1405/1496-1497.

results by alignment of the tRNA anticodon with bases around C1400 and alignment of mRNA with the 1500 region. This arrangement is stablized by coaxial-stacking of the rRNA (Figure 1).

The configuration of the decoding site in the above model requires that the two conserved strands be juxtaposed and anti-parallel. Although previously undetected in the secondary structure model, this arrangement is supported by comparative sequence data. Several possible base-pairs between the two regions have been suggested because they are invarient or co-varient. Two of these base-pairs (1394-1395/1505-1506) have recently been implicated in a conformational change between the active and inactive forms of the 30S subunit (Moazed et al., 1986b).

Experimental Design

It is evident from the descriptions above that the decoding region is a major functional domain of the protein biosynthesis apparatus. The complex interactions at this site are intriguing to study because of their importance in understanding the ribosome.

The fact that the conserved regions of the 3' end are single stranded not only implies they are available for binding of substrate, but suggests they may be available for binding of complementary oligonucleotide probes. Assaying for disruption of function by small oligomers is advantageous in that discrete sites can be probed--unlike chemical modifica-

tion or nuclease digestion in which all susceptible bases of the rRNA are attacked. By keeping the probes small, disruption of structure is limited.

Complementary DNA probes are easily synthesized, are stable and are obtainable in very pure form. The use of DNA also allows for a convenient assay for site specificity. Cleavage of the rRNA from the rRNA/cDNA hybrid by RNase H *in situ* will generate two rRNA fragments. Generation of the correct sized fragments verifies the site of probe binding. Isolation and sequence analysis of one of the fragments provides further verification.

Probe binding can be monitored by filter binding assays. Nitrocellulose filters bind proteins, but not nucleic acids. Therefore, the extent of probe hybidization can be calculated from the counts retained on a nitrocellulose filter after a hybridization reaction has been washed through. Competition for a specific binding site between probe and factors such as tRNA or mRNA can easily be followed in this way.

For these reasons, complementary oligonucleotide probing was used in this study as the method of choice for examination of the interactions at the 1500 conserved region.

Problem Studied

The fact that the single-stranded regions around bases 1400 and 1500 are highly conserved suggests a function central to the protein biosynthesis apparatus. Placement of these two regions within the decoding site further accentuates their

importance. The establishment of a tRNA interaction within the 1400 conserved region has been effectively verified by cDNA probing (Hill and Tassanakajohn, 1987). However, the interactions within the 1500 conserved region heve not been previously addressed in a cohesive manner.

The study described here investigated the structure and function of the conserved single-strand region of E. coli 16S rRNA between bases 1492 and 1506. Several interactions central to protein biosynthesis have been proposed for this region and have been investigated here by competition studies with complementary oligonucleotide probes. The specific interactions investigated are outlined below:

active/inactive transformation As first described by Zamir and co-workers (Zamir et al., 1969,1971,1974; Vogel et al., 1970; Ginzburg et al., 1973), inactive subunits are defined by their inability to bind polyuridylic acid (poly U) directed $tRNA^{Phe}$. Such subunits can be reactivated by heating in the presence of high Mg^{2+} concentrations. Recently, this inactive/active transformation was suggested to be accompanied by the formation of two sets of base pairs (923-927/1390-1393 and 1394-1395/1505-1506) (Moazed et al., 1986b). This transformation was investigated by determining the accessibility of the probe target site (bases 1492-1506) in the active and inactive forms.

mRNA and tRNA binding The apparent juxtaposition of the 1400 and 1500 conserved regions required to account for the

formation of the active form base pair sets is supported by other potential base-pairings between the two regions (Noller et al., 1986). The known interaction of tRNA anticodon with the 1400 region suggests an interaction of mRNA with the 1500 region to accomodate the codon/anticodon interaction (figure 1). The possibility of such a conformation was probed with cDNA oligomers in the presence and absence of poly U in both the inactive and active forms. The region was also probed when poly U directed $tRNA^{Phe}$ was bound to active subunits

IF-3 binding The differential nuclease digestion patterns of the colicin fragment (bases 1493-1542) in the presence of IF-3 in solution (Wickstrom, 1983) indicates that IF-3 binds to the 3' end of 16S rRNA and specifically interacts with bases 1498-1506. Competition studies between IF-3 and a cDNA oligomer targeted to the 1500 region was carried out to investigate this interaction.

The subunit anti-association activity of IF-3 was also investigated as a corollary to this study by cDNA/IF-3 competition at the 790 loop of 16S rRNA. A previous cDNA probing study (Tapprich and Hill, 1986) showed that the 790 loop plays an integral role in subunit association.

A model for the interactions of the 1500 conserved region based on the results of this study and other available data is presented and discussed. In addition, the results of this study are discussed in relation to defining the parameters of the cDNA probing technique.

Chapter 2

MATERIALS AND METHODS

Materials Frozen E. coli MRE600 cells were from Grain Processing Corp. (Muscatine, Iowa). RNase H was acquired from Promega Biotec (Madison, Wisc.) or Pharmacia (Piscataway, N.J.). T4 polynucleotide kinase was from either Pharmacia or United States Biochemicals (Cleveland, Ohio). New England Nuclear was the source of ^{32}P-gamma-ATP and IF-3 was the kind gifts of Dr. Albert Wahba at the University of Mississippi and Dr. John Hershey of the University of California, Davis.

Isolation of ribosomal subunits Isolation and purification of ribosomal subunits was carried out basically as described previously (Hill et al., 1969) except freshly grown log phase cells were used. E. coli MRE 600 cells were grown to mid log phase (optical density of 0.5 at 600nm) in 2 liter batches of trypticase soy broth (BBL) in 4 liter flasks. Aeration was provided by shaker table in a 37°C incubator. Each flask was inoculated with 2 ml of an overnight culture started from frozen cells. The cells were harvested by spinning 5 minutes at 5 K in a Sorval GSA rotor. Pellets were combined and stored no more than two days at -70°C.

Forty to fifty grams of cells were disrupted by grinding with 2X weight of alumina at 4°C in buffer A (10mM Tris-HCl pH 7.4, 200mM KCl, 10 mM $MgCl_2$) for 1 hour. The cell paste was then suspended in 200 ml of buffer A and the alumina removed by spinning 5 minutes at 5 K rpm. The alumina pellets were

washed by resuspending in 50 ml buffer A and spun again. The two resulting supernatants were combined and centrifuged for 1 hour at 16 K rpm to remove whole cells, cellular debris and alumina. The low speed supernatant containing 70S ribosomes was centrifuged in a Beckman Ti 70 rotor at 60 K rpm for 2.5 hours, resuspended in 50 ml of buffer A by gently stirring in cold room for 5 hours and again subjected to the low and high speed centrifugations to further purify the ribosomes.

The 70S ribosomes were dissociated into 30S and 50S subunits by resuspending the second high speed pellets in 30-50 buffer (10mM Tris-HCl pH 7.4, 100mM KCl, 1.5mM $MgCl_2$) and stirring gently overnight at 4°C. Subunits were then separated by zonal centrifugation in a Beckman Ti 15 rotor as outlined by Tam and Hill (1981). Fractions corresponding to the 30S peak were then pelleted by spinning in a Ti 70 rotor for 13 hours at 60 K rpm. The 30S subunits were washed in high salt to remove transiently bound proteins by resuspending the pellets in 5 ml SW buffer (0.5 M NH_3Cl, 10mM Tris-HCl pH 7.4, 15mM $Mg(OAc)_2$, 1mM DTT) overnight. The resulting suspension was centrifuged through a 20% sucrose cushion in SW buffer for 13 hours at 60 K rpm. The 30S pellet was then resuspended in 1 ml of 30-50 buffer and stored in 50 µl aliquots at -70°C.

Cell pellets were thawed only once and the entire cracking procedure from cells to subunits was carried out in a minimum of time. Subunits isolated in this manner showed

less degredation than those obtained from purchased frozen cells as determined by polyacrylamide gell electrophoresis of isolated rRNA (data not shown).

Ribosomes and ribosomal subunits were routinely checked for homogeneity by analytical ultracentrifugation. Only subunits showing well defined peaks were used in this study, although subunit degradation during isolation was a rare occurrance.

Preparation of probes The oligodeoxynucleotide probes used in this study were synthesized on a Biosearch 8600 automated DNA synthesizer using β-cyanoethylphosphoramidite chemistry on a 1 μmol scale. Probe 1492-1506 (dACCTTGTTACGACTT) was complementary to bases 1492-1506 and probe 1498-1506 (dACCTTGTTA) was complementary to bases 1498-1506 (Figure 2). The tritylated (5'-DMT) oligomers were removed from the solid support by incubating the synthesis column in concentrated NH_4Cl for 1-3 hours at room temperature. Benzoyl blocking groups were removed from the probes by further incubation with fresh concentrated NH_4Cl for 5 hours at 55°C in a sealed ampule. The DMT-oligomers were dried under vacuum, resuspended in 100 μl dH_2O and purified by reverse-phase HPLC (Figure 3a) on a 25 cm Column Engineering 10 μm ODS column. Separation of DMT-oligomers from default sequences was accomplished with a 20 minute HPLC gradient at 1 ml/min. The gradient was 100% buffer A (1mM TEA-OAc pH 7.3) to 70.8% buffer B (50% buffer A, 50% HPLC grade acetonitrile). The

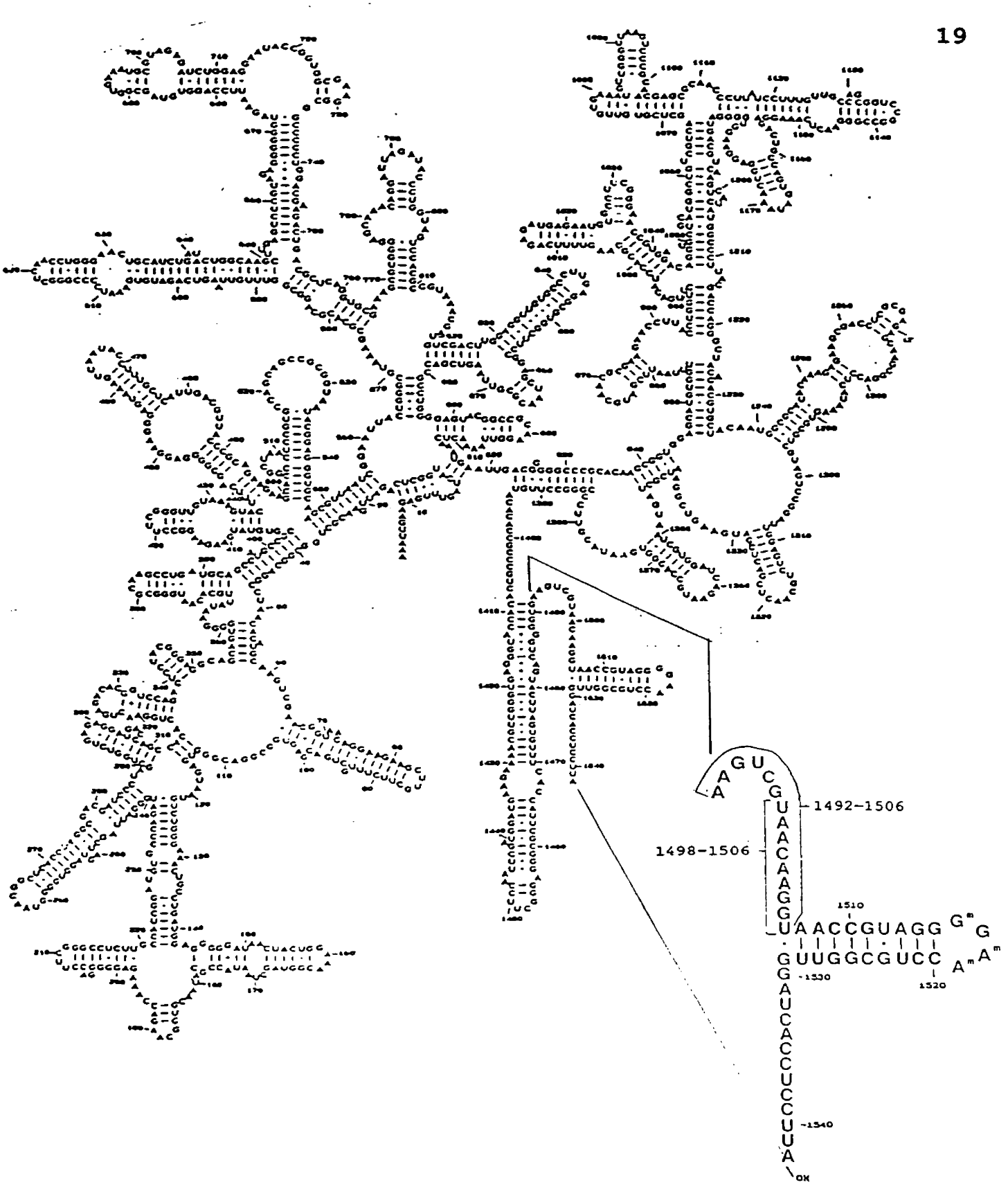

Figure 2 Probe Target Sites. Secondary structure map of E. coli 16S rRNA showing regions complementary to oligonucleotide probes (Noller et al., 1986).

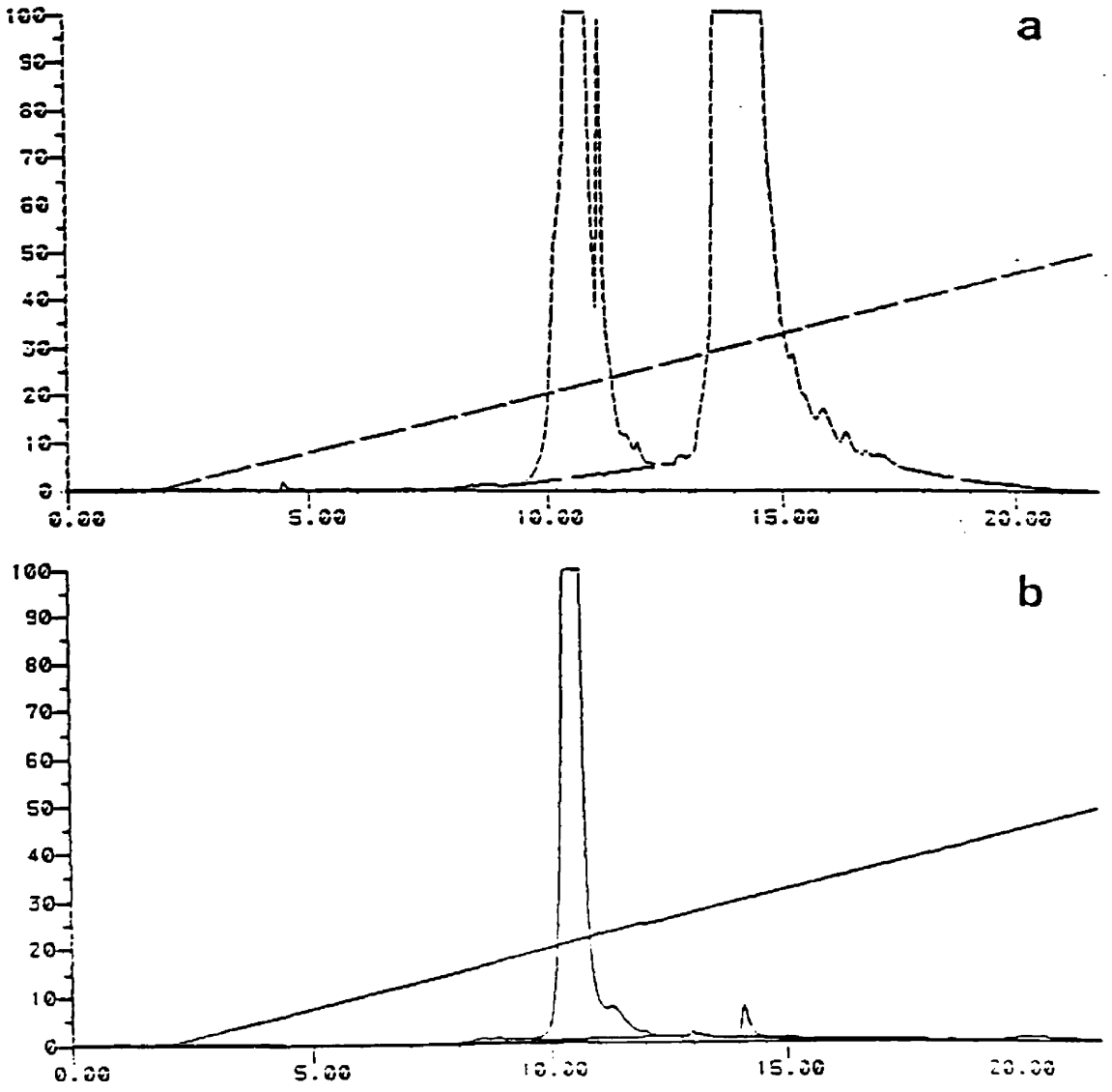

Figure 3 HPLC profiles of Oligonucleotide Work-up. a. Representative HPLC profile of DMT-oligomer. The peak at 10 minutes probably represents non-DMT-DNA and default sequences. The peak between 13.5 and 15.2 minutes was collected, the DMT blocking group removed, followed by a second HPLC run (b). The peak between 10-11 minutes was collected and used for probing studies. The abscissa is retention time in minutes. The ordinate is absorbance at 260nm (1 O.D. full scale).

DMT-probes were evaporated to dryness, resuspended in 1 ml of 80% acetic acid and incubated for one hour at room temperature to remove the 5′ trityl group. The detritylated probe was then again purified by HPLC as described (Figure 3b). Such probes were resuspended in water and the concentration determined by absorbance at 260nm with an extinction coefficient of 30 ml/mg·cm. The purity of the probes was checked by resuspending 20 µg of dried probe in 10 µl of loading buffer (8M urea, 0.025% xylene cyanol, 0.025% bromphenol blue) and running on a 20% polyacrylamide gel (12.5 cm X 13.5 cm X 1.5 mm) for 50 minutes at a constant 40 mAmps in TBE buffer (89mM Tris-borate pH 8.3, 1mM EDTA). Bands were visualized by staining with 0.2% methylene blue, 200mM acetic acid and 200mM sodium acetate followed by destaining with water.

Probes were 5′ end labeled with ^{32}P-gamma-ATP basically by the method of Maxam and Gilbert (1980). Reactions contained 35 pmol oligonucleotide, 35 pmol ^{32}P-gamma-ATP (3000 Ci/mmol) and 4 units of T4 polynucleotide kinase in a total volume of 50 µl of labeling buffer (50mM Tris-HCl pH 7.6, 10mM $MgCl_2$, 10mM DTT). Labeling reactions were incubated at 37°C for 30-45 minutes and stopped by the addition of 5 µl 200mM EDTA. Reactions were extracted once with an equal volume of buffer equilibrated phenol, the aqueous phase removed and saved followed by back-extraction of the organic phase 3-4 times with TNE buffer (10mM Tris-HCl pH 8.8, 100mM NaCl, 5mM EDTA). The back-extractions were combined with the original

aqueous phase and loaded onto NACS Prepac nucleic acid purification columns (Bethesda Research Laboratories), washed with low-salt buffer and eluted from the column with high-salt buffer as recommended by the manufacturer. Typically, probe recovery was about 70% as measured by radioactive partitioning before and after elution from the column (measured with Geiger counter). The specific activity of probes thus isolated was generally about 6.0 x 10^6 cpm/pmol.

Radiolabeled probes were also monitored for purity on polyacrylamide gels as described above except 100,000-300,000 cpm of probe was loaded. After 45 minutes, the electrophoresis was halted and a second sample was loaded in an adjacent lane. Power was again applied to the gel and allowed to run another 5 minutes. This second loading was used to determine if any unicorporated ^{32}P was still present in the probe preparations. Bands were visualized by autoradiography for 15-30 minutes with Kodak XAR-5 film. As can be seen in Figure 4, the oligomers migrate as a single band. The ability of these oligomers to be 5′ end-labeled also indicates structural integrity in that the oligomer can act as a substrate for polynucleotide kinase.

Gradient binding assays Probes were bound to the 30S subunit by incubating two A_{260} units of subunits with 100,000-300,000 cpm of labeled probe in binding buffer (10mM Tris-HCl pH 7.4, 60mM KCl, 10mM $MgCl_2$) for 30 min. and then layering on a 4 ml 5-20% sucrose gradient in the same buffer. Assays were

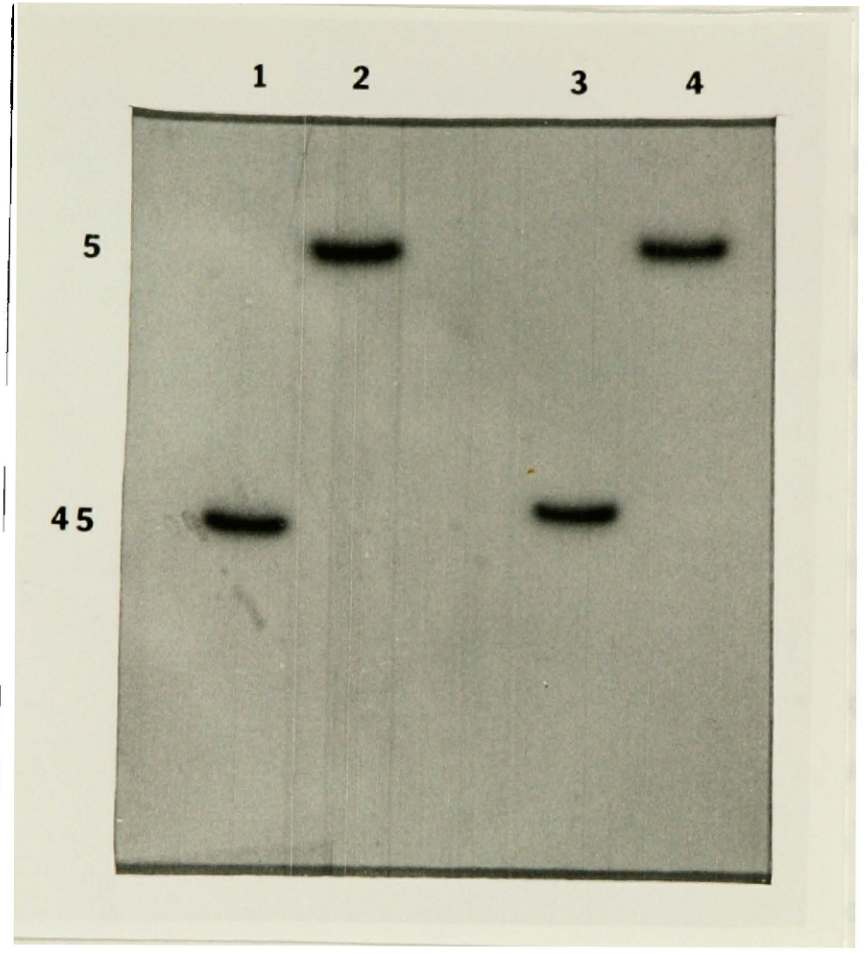

Figure 4 Autoradiogram of ^{32}P Labeled Oligomers. Probes 1498-1506 and 787-795 were electrophoresed for 5 and 45 minutes on a 20% acrylamide-urea gel. The second loading indicates that the oligomers have been purified away from unincorporated label. Lanes 1 and 2-probe 1498-1506; lanes 3 and 4-probe 787-795.

centrifuged 2 hours at 54 K rpm in a Beckman SW60 rotor. The gradients were fractionated, the subunit peak determined spectrophotometrically and the probe migration determined by liquid scintillation counting.

Filter binding assays Binding reactions were also assayed by filtering through nitrocellulose filters. Fifty µl reactions containing 25-50 pmol of 30S subunits and increasing amounts of labeled probe (SA= 400-1000 cpm/pmol) in hybridization buffer (10mM Tris-HCl pH 7.4, 100mM KCl, 5mM $MgCl_2$) were incubated for 0.5-20 hours at 4°C and then spotted onto nitrocellulose filters (Millipore HAWP 0.45 µm). The filters were washed five times with 1 ml of cold buffer under low vacuum. After drying, the filters were counted by liquid scintillation. For each reaction done in this manner, a control reaction containing all components except subunits was also done. The extent of probe binding was then determined by subtracting the background counts of the control filter from the counts retained on the corresponding reaction filter.

RNase H assays Verification of the site of cDNA probe binding was carried out by incubating 20 µg of 30S subunits with a two molar excess of probe (about 44 pmol) and 3 units of RNase H for 18 hours at 4°C. Reactions were then extracted 2-3 times with buffer equilibrated phenol, precipitated with two volumes of 95% EtOH at -70°C for at least one hour. The precipitated RNA was pelleted by centrifuging at 12,000 X g for 1 hour. The pellets were washed once by layering 1 ml of 70% EtOH over

the pellets and respun for 0.5 hours. Pellets were resuspended in loading buffer (8M urea, 0.025% xylene cyanol, 0.025% bromphenol blue), heated and quick-cooled, layered on a 6% polyacrylamide, 7M urea gel and electrophoresed 2.5 hours at 12.5 mAmps. RNA bands were then visualized by staining with methylene blue.

When a RNase H fragment was to be sequenced, the gel was not stained, but instead visualized by UV shadowing and the RNase H fragment removed. RNA was eluted from the gel slice by maceration and soaking in elution buffer (500mM NH_4OAc, 10mM $Mg(OAc)_2$, 1mM EDTA, 1% SDS) as described by Maxam and Gilbert (1980). Following separation of eluted RNA from the gel paste by centrifugation through glass wool, the RNase H fragment was precipitated by addition of two volumes of 95% EtOH and incubated at -70°C for at least 1 hour. The precipitate was then pelleted by centrifugation at 12,000 X g for 1 hour then the ammonium salt was removed by resuspending the pellet in 0.5 ml of 100mM NaOAc and reprecipitating. The final pellet was resuspended in water and stored at -20°C in two volumes of 95% EtOH.

Reverse Transcriptase Sequencing The exact site of probe directed RNase H cleavage was determined by primer extension sequence analysis of the gel purified RNase H fragment. A ten base primer complementary to bases 1533-1542 was synthesized as described and hybridized with the RNase H fragment. Hybridization reactions contained 5 pmol fragment and 10 pmol

Table I N° solutions for reverse transcriptase sequence analysis. Solutions contain 50mM Tris-HCl pH 8.0, 50mM KCl and 10mM $MgCl_2$.

	concentrations in µM			
mix:	A°	C°	G°	T°
nucleotide				
ddATP	-	-	-	0.5
ddCTP	-	-	100	-
ddGTP	-	100	-	-
ddTTP	100	-	-	-
dCTP	100	100	100	100
dGTP	100	100	100	100
dTTP	100	100	100	100

primer in hybridization buffer (50mM Tris-HCl pH 8.0, 100mM KCl, 20mM $MgCl_2$) in a total volume of 10 µl. This mixture was incubated at 90°C for 1 minute and allowed to cool to room temperature. The hybridization mixture was then split into four equal portions, one for each of the four dideoxy nucleotide mixtures (N° solutions, table I). To each of these tubes, 2 µl of hot mix (2 U/µl AMV reverse transcriptase, 50mM Tris-HCl pH 8.0, 50mM KCl, 10mM $MgCl_2$, 10 µCi α-^{35}S-ATP) and 5 µl of the corresponding N° solution was added. After 30 minutes at 42°C, 5 µl of chase mixture (1 U/µl AMV reverse transcriptase, 50mM Tris-HCl pH 8.0, 2mM DTT, 1.2mM each dATP, dCTP, dGTP, dTTP, 10% (v/v) glycerol) was added followed by 15 minutes further incubation at 42°C. The reactions were stopped by the addition of 5µl loading buffer (80% (v/v) deionized formamide, 50mM Tris-borate pH 8.3, 1mM EDTA, 0.1% (w/v) xylene cyanol, 0.1% (w/v) bromphenol blue), incubated for 3 minutes at 95°C and quick-cooled on ice. Five µl of each reaction was then loaded onto a 10% polyacrylamide, 7M

urea sequencing gel (10% (w/v) acrylamide, 0.5% (w/v) methylene bis-acrylamide, 7M urea, 0.1% (w/v) ammonium persulfate, 0.04% (v/v) TEMED, 50mM Tris-borate pH 8.3, 1mM EDTA) and electrophoresed 2 hours in TBE buffer at a constant 60 watts. The gel was removed from the glass plates and fixed for 15 minutes in 2 liters of a 5% acetic acid, 5% methanol solution and dried onto a sheet of filter paper (Whatman 3mm). The sequence was visualized by exposing Kodak XAR-5 film for 24 hours.

Active/Inactive Competition Assays Subunits were brought to 20mM Mg^{2+} by the addition of the appropriate amount of 1M $MgCl_2$ and the subunits divided into two equal portions. One portion was kept cold (inactive sample) and the other portion incubated at 40°C for 20 minutes (active sample). Activation was verified by testing non-enzymatic poly-U directed ^{14}C-Phe-$tRNA^{Phe}$ binding (Zamir et al., 1971). Probe binding to the two states was then determined as for filter binding assays. Reactions typically contained 30-50 pmol active or inactive subunits and a 2,6,12,18,24 and 30 molar excess of labeled probe (SA=500 cpm/pmol).

mRNA and tRNA Competition Assays Probe competition experiments with poly U were carried out by pre-binding about 20 µg poly U (Sigma, MW=100,000~300 bases/strand) to 50 pmol of active or inactive subunits at 4°C for 10 minutes. Reactions were then carried out as for filter binding assays using 2,6,12,18,24 and 30 molar ratio of probe/subunit (SA=500

cpm/pmol). Control reactions without subunits contained 20 µg poly U.

For competition assays with tRNA, reactions with active subunits were set-up as for mRNA assays with the addition of 75 pmol $tRNA^{Phe}$ (Boerhinger Mannheim Biochemicals) to the pre-incubation mixture. Control reactions also contained tRNA.

Reductive Methylation of IF-3 In order to determine that IF-3 binds to 30S subunits under the conditions used for hybridization, IF-3 was first labeled with ^{14}C by reductive methylation (Benne et al., 1981). Dialysis of 400 µg IF-3 in 200 µl total volume was carried out for 12 hours at 4°C with several buffer changes of buffer B (100mM Na-borate pH 9.0, 300mM KCl, 5mM BME). Immediately before reduction, 1 mg of $NaBH_4$ was dissolved in 1 ml of ice-cold dH_20 and placed on ice. Dialyzed IF-3 was then placed into a glass reaction tube and 50 µl ^{14}C-formaldehyde (250 µCi at 45 mCi/mmol) was added. The reaction was vortexed 2 seconds and placed on ice for 60 seconds. Forty µl of the freshly made $NaBH_4$ solution was added, the reaction vortexed for 2 seconds and then immediately placed into a dialysis bag and dialyzed against several 2 liter changes of hybridization buffer to remove unincorporated radioactivity.

To assay the ability of IF-3 to bind 30S subunits, roughly equimolar amounts of labeled IF-3 (about 4 pmols, 2000 cpm/pmol) and subunits (4 mg) were incubated for 20 minutes at 37°C in 100µl total volume of hybridization buffer. This

reaction was layered onto a 13 ml 5–20% sucrose gradient, also in hybridization buffer, and centrifuged 5.5 hours at 37 K rpm (4°C) in a Beckman SW41 rotor. A control reaction containing the labeled IF-3, but no subunits was also centrifuged. The gradients were fractionated (400 µl fractions), subunit migration determined spectrophotometrically and IF-3 migration by scintillation counting.

IF-3 Competition Assays The effect of IF-3 on probe binding was investigated by pre-incubating 60 pmol unlabeled IF-3 with 30 pmol inactive subunits for 20 minutes at 37°C in hybridization buffer. Reactions were then carried out as for filter binding assays with control reactions also containing 60 pmol IF-3. In a similar manner, a mock reaction was carried out using 60 pmol α-chymotrypsinogen A instead of IF-3. To analyze the ability of IF-3 to displace pre-bound probe, increasing amounts of IF-3 were added to filter binding reactions containing 30 pmol inactive subunits and 400 pmol labeled probe (SA=500 cpm/pmol). Reactions were then treated as for filter binding assays and control reactions contained all components except subunits.

Subunit Association Assays The ability of isolated subunits to form 70S ribosomes was tested by incubating equimolar (200 pmol) amounts of 50S and 30S subunits in 100 µl association buffer (20mM Tris-HCl pH 7.4, 60mM KCl, 10mM $MgCl_2$) for 45 minutes at 37°C. These reactions were layered onto a 13 ml 5–20% sucrose gradient and centrifuged at 37 K rpm at 4°C for

4.5 hours in an SW41 rotor. Approximately 500 µl fractions were collected and migration determined by spectrophotometric analysis at 260 nm.

When the subunit anti-association activity of IF-3 was tested, control reactions were set-up as described above and test reactions contained 200 pmol 30S subunits that had been preincubated at 37°C for 15 minutes with 300 pmol IF-3. Similarly, when probe 16S(1498)-9 was tested in subunit association assays, the same procedure was carried out except test reactions contained 3200 pmol unlabeled probe and instead of using the entire 100 µl reaction, a 50 µl aliquot of the test and control reactions were layered onto a 2 ml 5-20% sucrose gradient and centrifuged at 55 K rpm for 50 minutes in a Beckman TL-55 rotor. Fractions of about 125 µl were then collected and migration analyzed at 260 nm.

Physical Methods Ribosome and ribosomal subunit homogeneity and integrity was routinely monitored by sedimentation velocity experiments carried out in a Spinco Model E analytical ultracentrifuge equipped with schlieren optics. Samples were generally 5-10 mg/ml and a total of 800 µl was loaded into a standard 14 mm sample cell. The samples were centrifuged at 52,000 rpm at 4°C in an ANH rotor. Schlieren patterns were analyzed visually for well defined peaks which indicated homogeneous, undegraded samples. Alternatively, photographs were taken at 4-8 minute intervals.

Diffusion coefficients of probe-subunit complexes were

obtained using quasi-elastic light scattering (QLS) (Bloomfield, 1981). Samples contained 200 µg of subunits and a 16 molar excess of probe in a total volume of 500 µl of hybridization buffer and were incubated for 2 hours at 4°C. Samples were centrifuged prior to scattering for 10 hours at 5000 rpm, 4°C in a Sorval HB-4 rotor to ensure a dust-free sample.

The correlation function was obtained using a Malvern 4300 spectrometer system and a Langely-Ford 1096 autocorrelator. Incident light was provided by a Lexel 4 watt argon ion laser. Analysis of the correlation functions to yield diffusion coefficients was carried out by the method of Blair et al. (1981).

Chapter 3

Results

The experiments described in this section were designed to investigate several proposed interactions within the conserved bases 1492–1506 in the 3′ region of E. coli 16S rRNA. To this end, two complementary oligodeoxyribonucleotides were synthesized and hybridized to isolated 30S subunits. The extent of probe binding under various conditions was used to probe the structure and function of the region.

Probe Binding

In situ hybridization of probes to subunits was first demonstrated by gradient binding assays. In this assay, hybridization reactions of 30S subunits and ^{32}P labeled oligomers were layered onto sucrose density gradients and centrifuged to separate bound subunits from unbound probe. Comigration of ^{32}P counts with 30S subunits indicates probe binding. Figure 5 shows a gradient binding assay of probe 1498–1506. Although gradient binding assays showed comigration of probe with subunits, binding was rarely more than 5% of the total added probe, far less than saturation. This may be due to the non-equilibrium conditions of the gradient. Because of the low binding, non-specific interactions cannot be ruled out.

A more quantitative indication of probe binding is seen in filter binding assays. The subunits in hybridization

mixtures spotted onto nitrocellulose filters are retained while excess probe is washed through. Determination of retained radioactivity by scintillation counting quantifies the probes bound to subunits. A filter binding curve obtained in this manner for probe 1498–1506 is presented in Figure 6. Typically, the curves saturated at 20–40% of the added subunits bound by probe. The fact that the curves saturates is a characteristic of site specific ligand interactions.

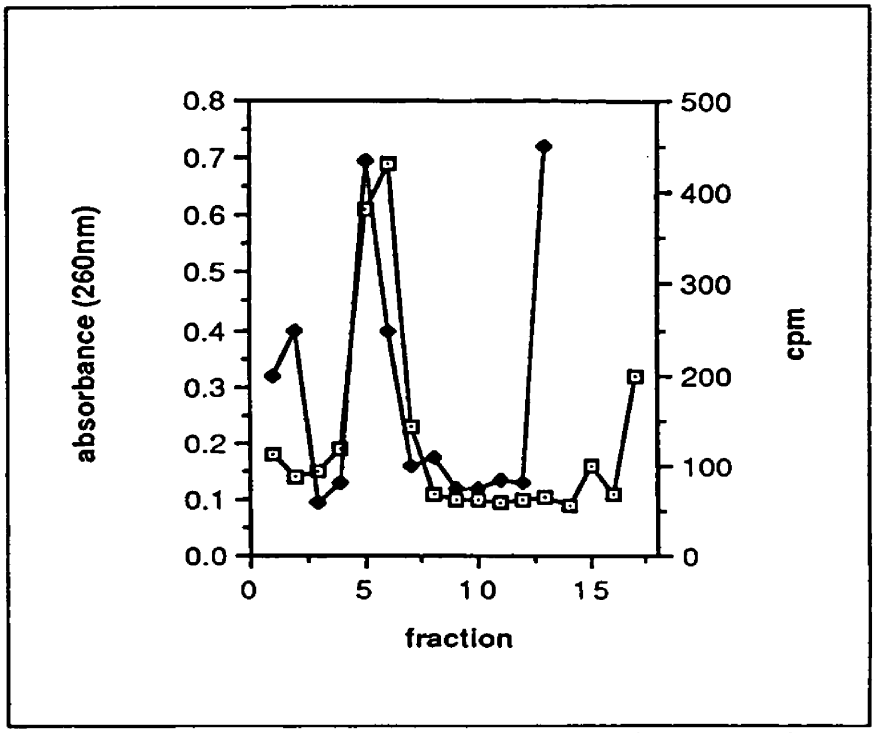

Figure 5 Probe 1498–1506 Gradient Binding Assay. Open boxes represent absorbance and closed boxes CPM.

Saturation levels for filter binding assays proved to vary under different conditions including vacuum pressure, hybridization time and lot number of filters used. Although care was taken to minimize such variables, any assay used to compare functional differences were carried out simultaneously under equivalent conditions. It is also important to note that any filter binding experiment reported here was repeated at least three times.

RNase H Assays

Indication of probe binding to 30S subunits is evident in gradient and filter binding assays. Neither assay, however, rules out specific binding to sites other than the target site, e.g. nucleic acid binding sites on the ribosomal proteins.

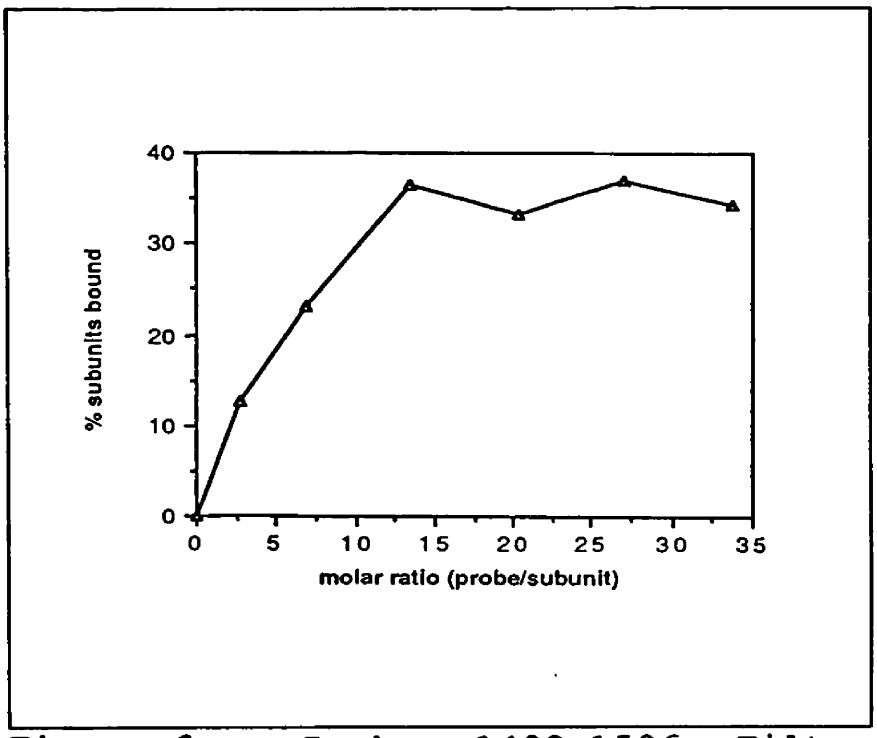

Figure 6 Probe 1498–1506 Filter Binding Assay. Each reaction contained 25 pmol salt-washed 30S subunits.

Definitive proof of target site specificity is shown in RNase H digestion studies. The general procedure of these assays was to use a two molar probe-to-subunit ratio under hybridization conditions and digest the rRNA of the resulting duplex with RNase H. After an empirically determined incubation time (Figure 7), the resulting fragments were separated on a polyacrylamide gel.

Figures 8 and 10 depict RNase H digestion patterns for probes 1498–1506 and 1492–1506. The appearance of the small band in lane g of Figure 8 and lane b of Figure 10 can only be attributed to digestion of a cDNA/rRNA duplex. Elution of the band from the gel followed by primer extension sequence

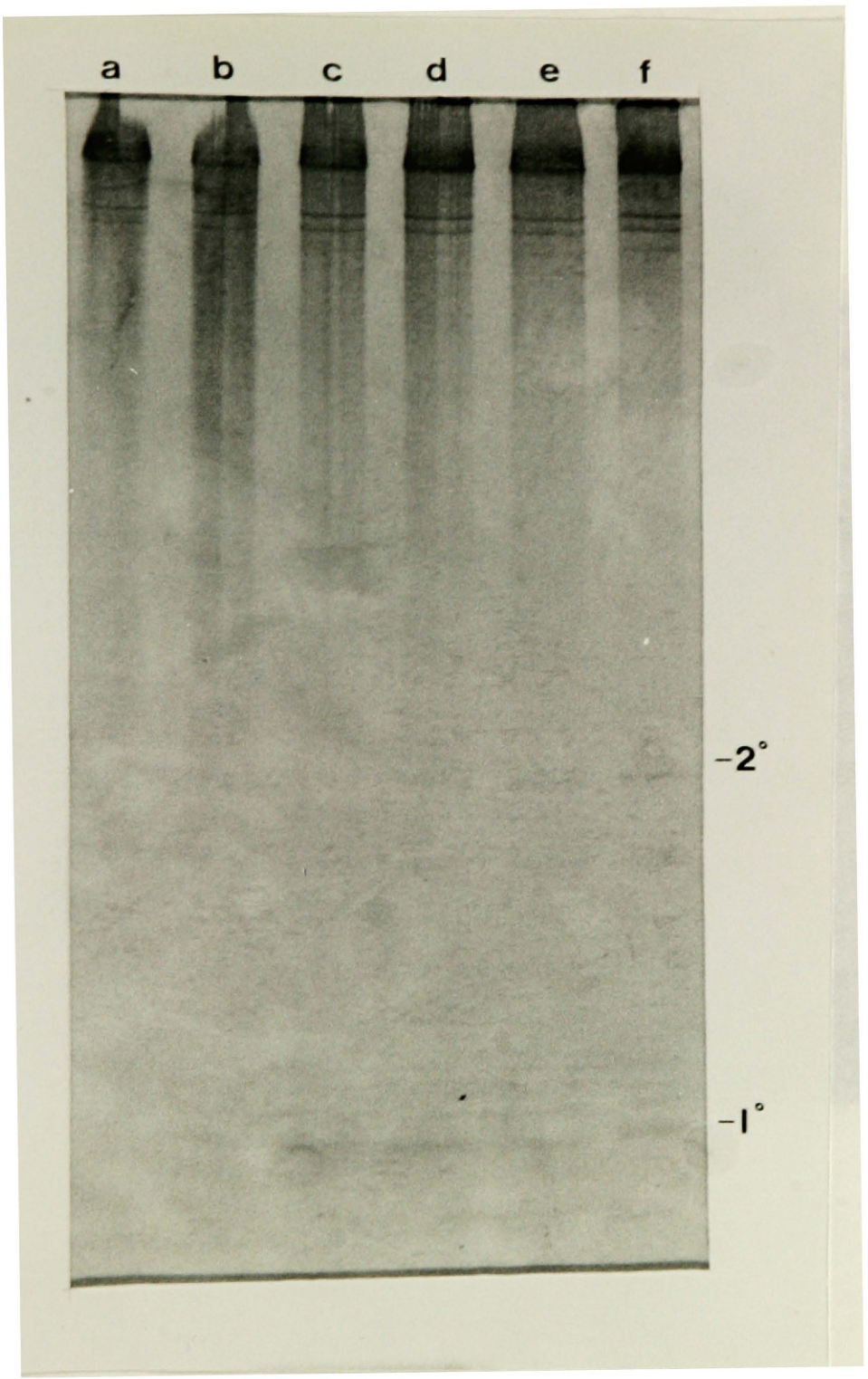

Figure 7 Probe 1492-1506 RNase H Time Titration. Lanes a-f are 0,6,12,24,36 and 48 hour incubations respectively. Primary and secondary cleavage products are marked.

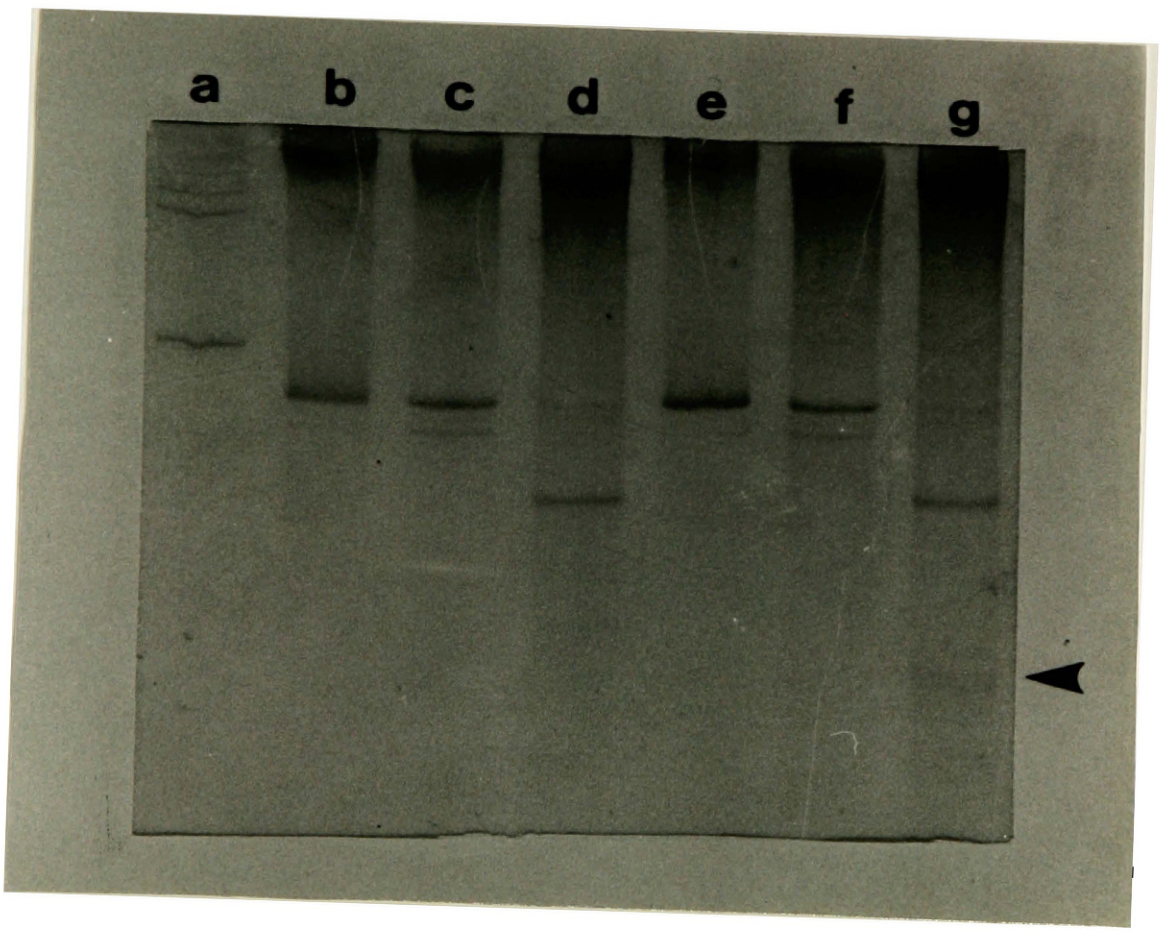

Figure 8 Probe 1498-1506 RNase H Assays a-RNA markers; b-70S control; c-50S control; d-30S control; e-70S+1498-1506; f-50S+1498-1506; g-30S+1498-1506. The arrow indicates the RNase H fragment in lane g.

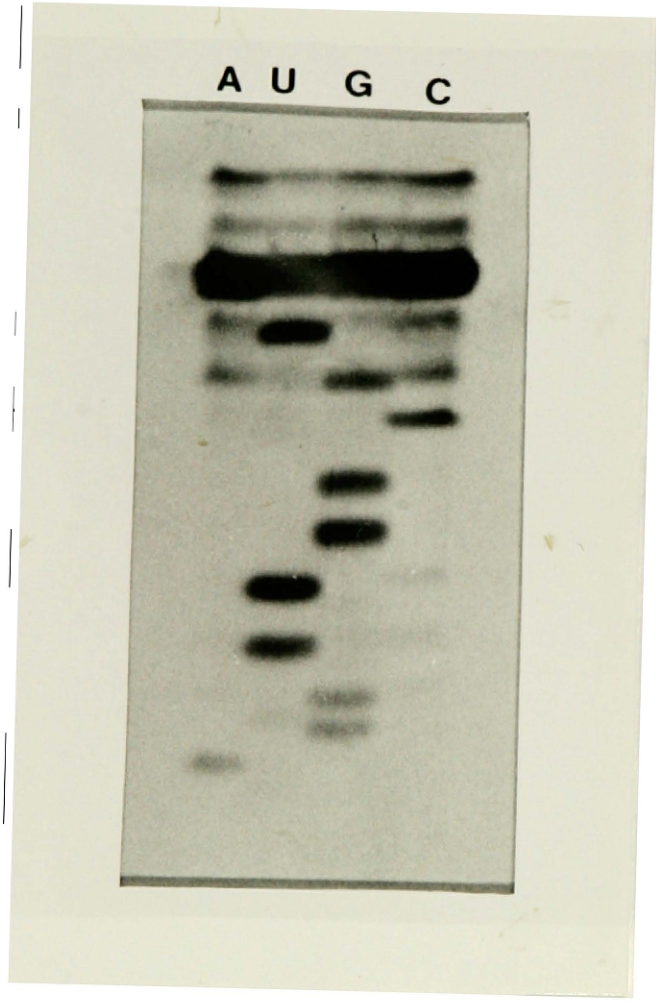

Figure 9 Probe 1498-1506 RNase H Fragment Sequence Analysis. Reverse transcriptase was used with a 10 nucleotide primer complementary to bases 1533-1542 in 16S rRNA.

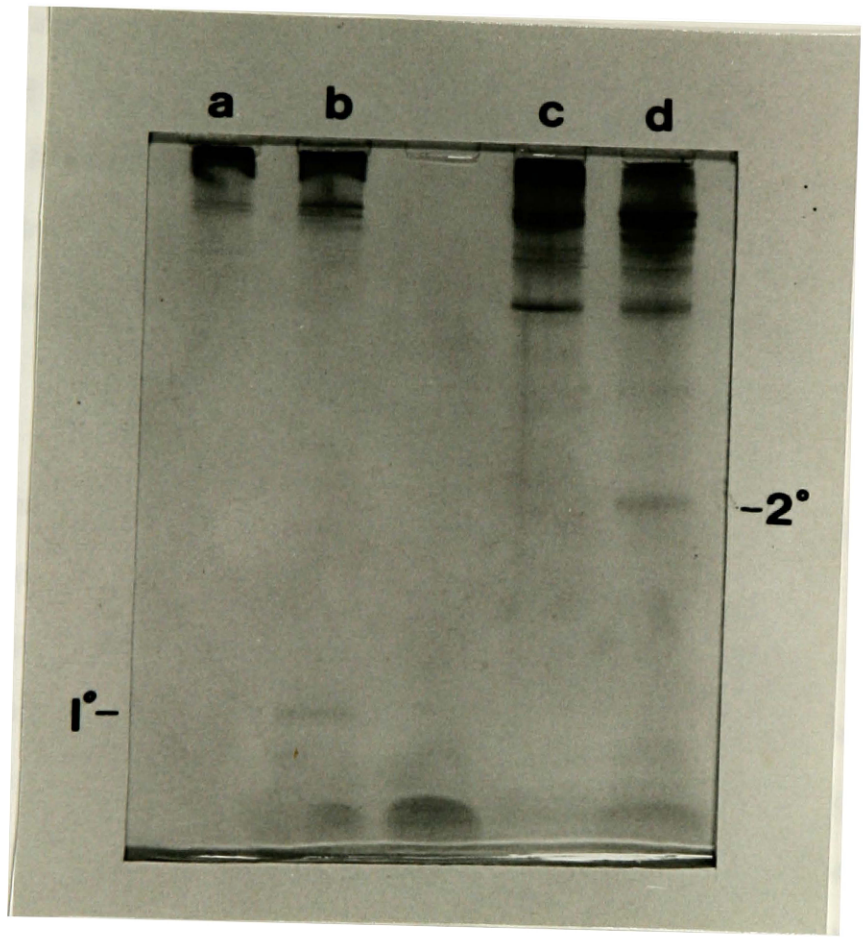

Figure 10 Probe 1492-1506 RNase H Assay. Comparison of native and unfolded subunits. a-native 30S only. b-native 30S+1492-1506. c-1492-1506 only. d-ion-depleted 30S only. e-ion-depleted 30S+1492-1506. 1°-primary cleavage fragment. 2°-secondary cleavage product.

analysis (Figure 9) indicates that this band is indeed the 3′ end of 16S rRNA. A characteristic of reverse transcriptase used in primer extension experiments is that the enzyme cannot read through modified bases easily and the sequence of the RNase H fragment shows pauses at the dimethyl adenines at bases 1518 and 1519. Even though this further establishes that the RNase H fragment is the 3′ end of 16S rRNA, the sequence does not establish the exact cutting site of RNase H. However, given that the fragments for both probes are the same size, it is likely that the heteroduplex was entirely digested.

The migration of the RNase H fragments in the expected size range and subsequent sequence analysis shows that the oligomer probes are indeed binding to their target sites. Examination of the RNase H gels, however, reveals other bands that appear to be less than 5% of the major digestion product and may represent secondary binding sites. A computer search for binding sites on the rRNA other than the target site indicated several partially homologous regions (table 2). With a few exceptions, these sites are five bases or less and most are found within double-stranded regions that are probably not readily available for probe binding. Of the exceptions, two are six base homologies (59-64 and 1332-1337) and three are 5 base homologies (260-264, 811-815 and 1179-1183). All of these regions are single stranded. In order to determine how this secondary homology might effect an RNase

Table II 16S rRNA/Probe Homology Regions

struc.-indicates the structural environment of the region (ss-single stranded; ds-double stranded)
H-indicates the potential for RNase H cleavage

bases	struc.	H	nucleotides
59-64	6ss	++	AAGUCG
260-264	5ss	+	GUAAC
569-573	4ss 1ds	-	CGUAA
595-599	1ss 4ds	-	AAGUC
659-663	5ds	-	UCGUA
811-815	5ss	+	CGUAA
872-877	1ss 5ds	-	AAGUCG
1061-1065	1ss 4ds	-	GUCGU
1092-1096	4ss 1ds	-	AAGUC
1196-1200	2ss 3ds	-	AAGUC
1294-1299	3ss 3ds	-	GUCGUA
1332-1337	6ss	++	AAGUCG
1505-1509	1ss 4ds	-	GUAAC
49-53	3ss 2ds	-	UAACA
69-74	2ss 4ds	-	GUAACA
899-904	3ss 3ds	-	CAAGGU
935-939	3ss 2ds	-	ACAAG
1179-1183	5ss	+	AAGGU
1498-1506	15ss	+++	AAGUCGUAACAAGGU

H assay, probe 1492-1506 digests of magnesium depleted, unfolded subunits were compared to digests of native subunits (Figure 10). Unexpectedly, the 3′ 36 base fragment was not generated with unfolded subunits, but instead a fragment of approximately 200 bases was evident. This fragment probably corresponds to cleavage at the 1300 region. Since this band is not apparent in the native digest, the potential pairing of probe to bases 1332-1337 probably does not contribute to overall binding to native subunits.

Probing Active and Inactive Subunits

Establishment of target site specific probe binding allows for analysis of probe binding data between different functional states. The above assays were carried out on 30S subunits that had been isolated and stored under the low salt conditions and shown to be in the inactive subunit conformation by ^{14}C-Phe-$tRNA^{Phe}$ binding (Zamir et al., 1974). By increasing the divalent salt concentration to 20mM and incubating a portion of these for 20 minutes at 40°C, the two different conformational states were obtained independent of salt concentration. This is basically the same procedure described by Moazed and co-workers (1986b) for reactivation of subunits. Filter binding assays carried out under these two conditions show a marked decrease in probe binding to active subunits for both the 9-mer and a smaller decrease for the 15-mer (Figure 11). These decreases are compatible with the proposed pairing of bases 1394/1395 and 1505/1506 upon

activation. The reduction of only 20% for probe 1492-1506 as compared to a 60% reduction for probe 1498-1506 may be indicative of the longer probe's ability to form a more stable hybrid with the target sequence when the two base pairs are formed upon activation.

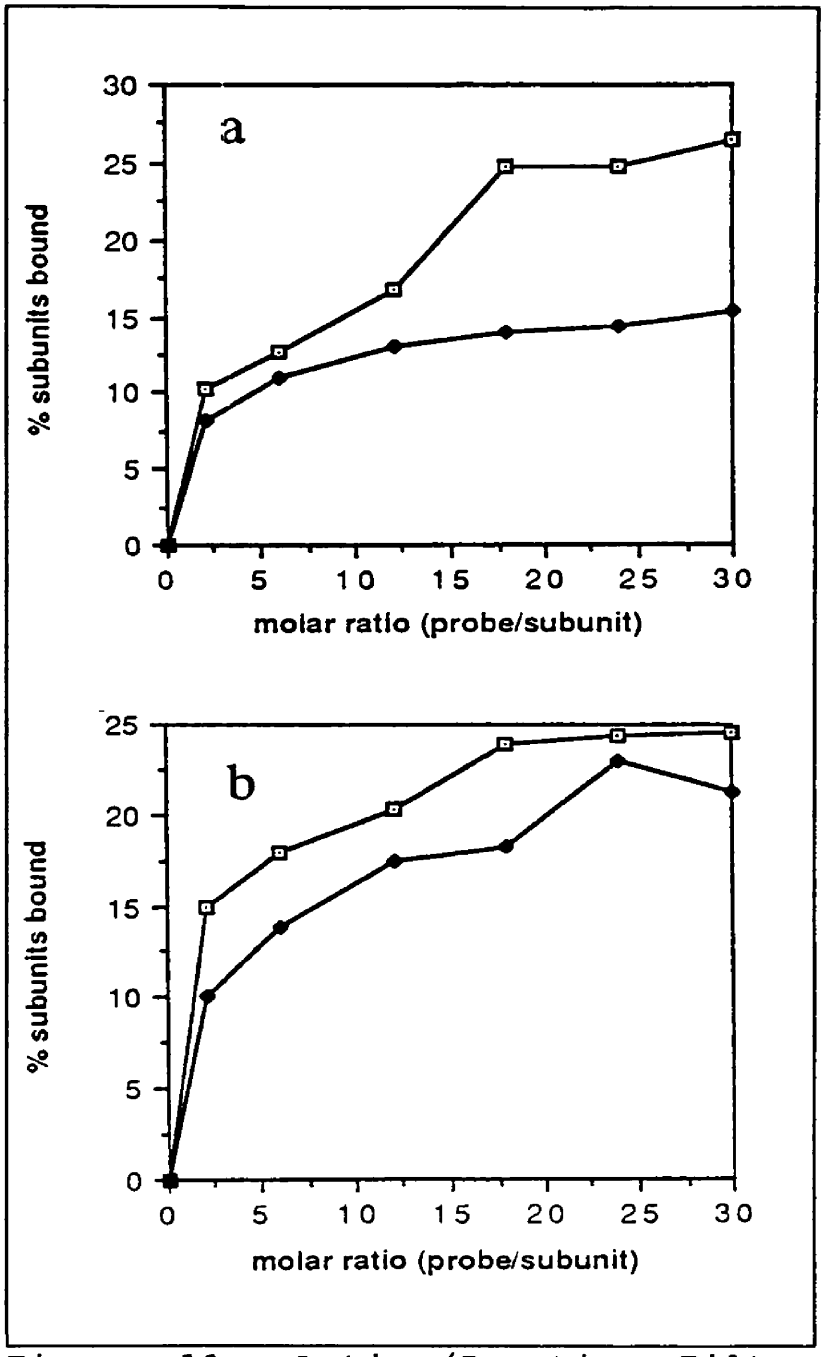

Figure 11 Active/Inactive Filter Binding Assays. a-probe 1498-1506. b-probe 1492-1506. squares-inactive. diamonds-active.

In an attempt to further probe the availability of the 1500 region, filter binding assays for both probes were carried out in which the hybridization mixtures (with probe present) were incubated at 37°C for 20 minutes before placing on ice. Binding curves thus obtained are indicated in Figure 12. Probe 1498-1506 binding to active subunits was basically the same as to inactive subunits, but

probe 1492-1506 showed a greater saturation level than with active subunits. This difference in binding suggests that the region between bases 1492 and 1497 is more accessible to probe binding upon co-incubation of probe and subunits at 37°C.

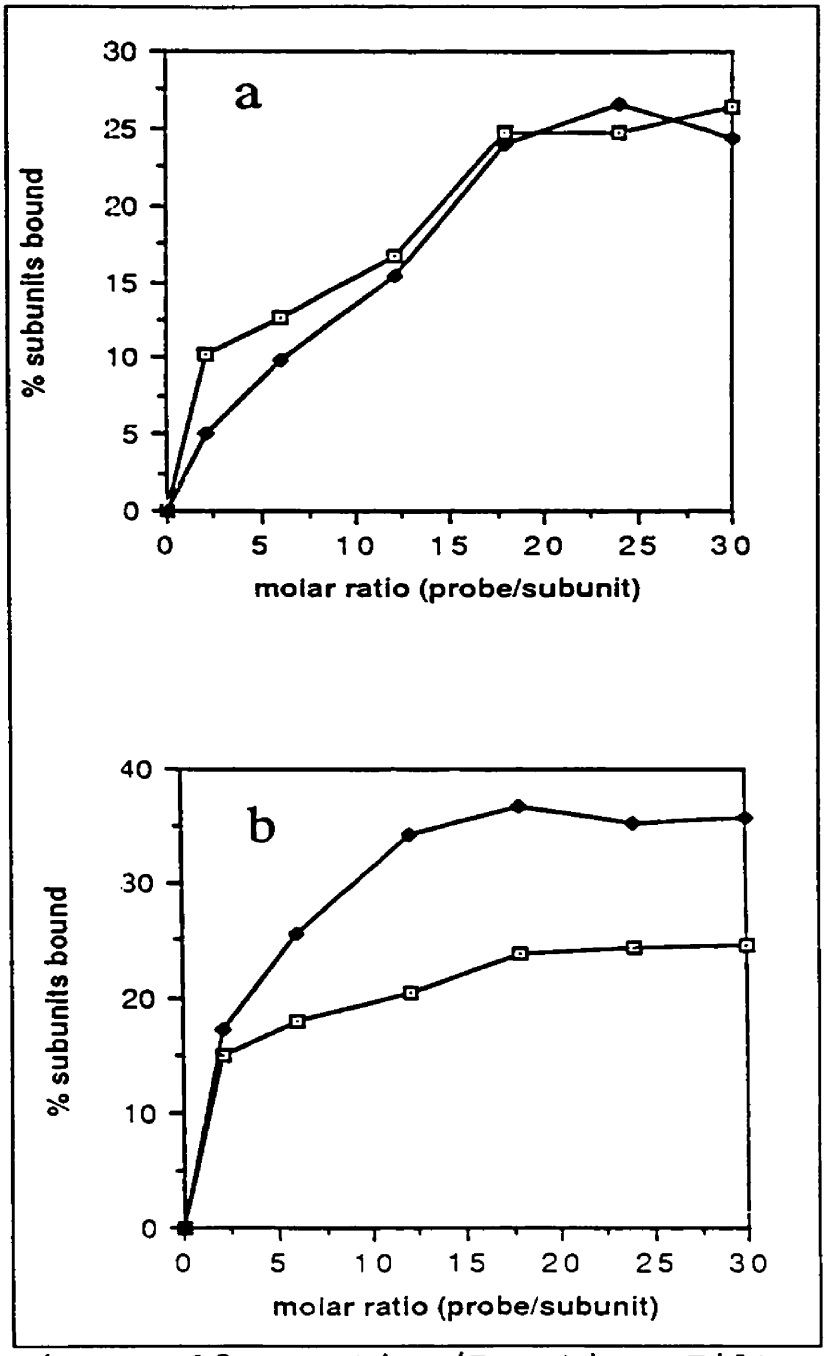

Figure 12 Active/Inactive Filter Binding Assays Co-incubated with Probe. a-probe 1498-1506. b-probe 1492-1506. squares-inactive. diamonds-activated with probe present.

Probing poly U interaction

The proposed base pairing of the active/inactive transformation requires a juxtaposition of the 1400 and 1500 conserved regions. The coaxial stacking model of tRNA binding at the 1400 region implies that mRNA be located near the 1500 region for the codon/anticodon interaction to occur (Noller et al., 1986). This possibility was tested by comparing probe 1498-1506 binding data in the presence and absence of the

synthetic mRNA poly uridylic acid (poly U). Subunits were prepared as described above to distinguish active and inactive conformations and preincubated (10 min. 4°C) in binding buffer with a two fold excess of poly U. To one set of reactions containing active subunits and poly U, a two fold excess of $tRNA^{Phe}$ was added. Probe binding was then carried out as for filter binding assays.

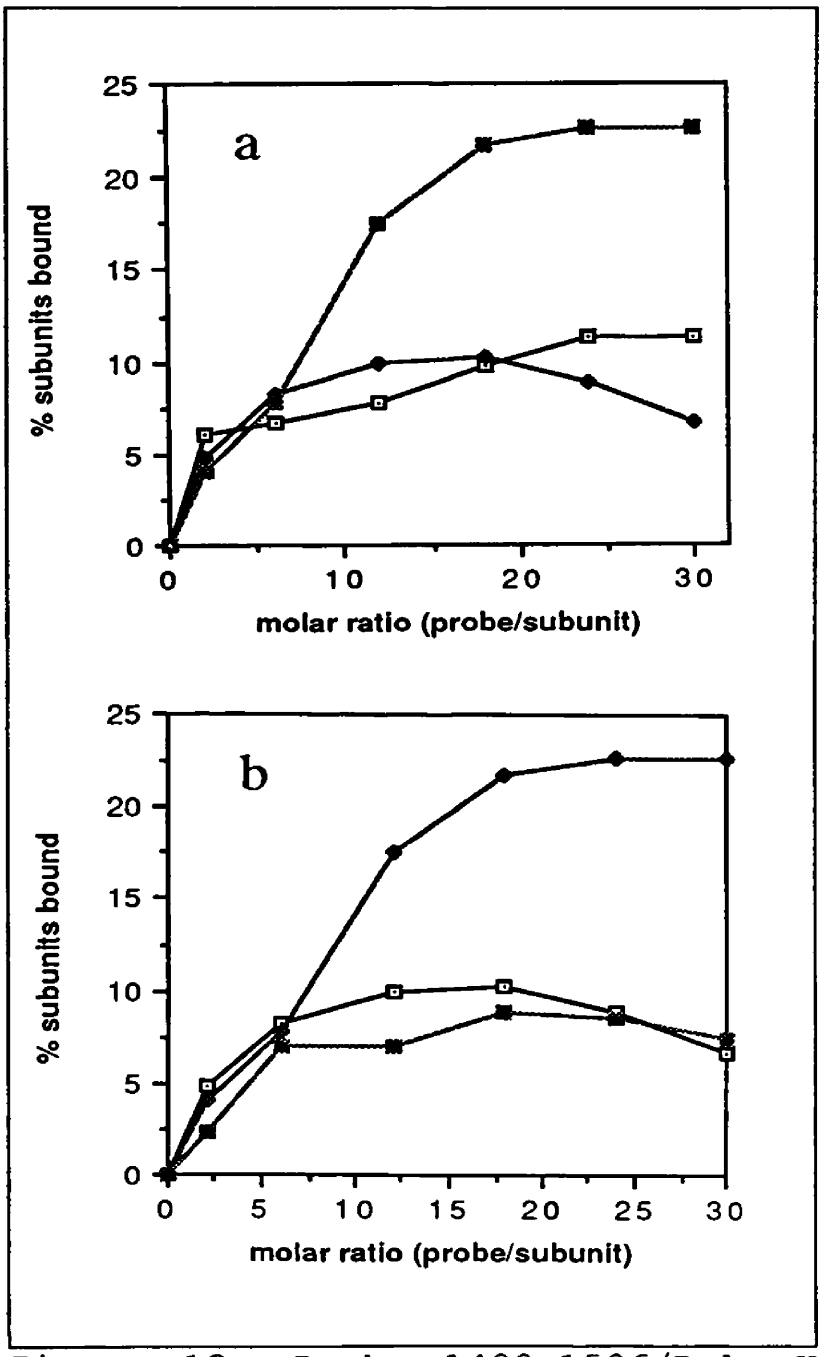

Figure 13 Probe 1498-1506/Poly U Filter Binding Assays. a. closed squares-inactive subunits, open squares-inactive+poly U, diamonds-active+poly U. b. diamonds-inactive, open squares-active+poly U, closed squares-inactive+poly U+tRNA.

As seen in Figure 13a, approximately an 80% decrease in probe 1498-1506 binding is evident for inactive subunits suggesting that the target site is unavailable for probe binding when poly U is bound. The same decrease was seen for both active and

inactive subunits as well as when $tRNA^{Phe}$ was bound (Figure 13b). When these data are compared to curves for active subunits alone, it is apparent that poly U has a greater effect on probe binding than activation of subunits.

Probing IF-3 interaction

One of the major functions proposed for IF-3 is to facilitate mRNA binding to the initiation complex. Differential accessibility of several bases within the 1498-1506 region upon IF-3 binding (Wickstrom, 1983) suggests that either IF-3 binds this region or causes a conformational change that would cause decreased cDNA probe binding. This interaction was investigated by several probing experiments.

To ensure that IF-3 binds to 30S subunits in the conditions used for probe hybridization, IF-3 was labeled with ^{14}C by reductive methylation and bound to 30S subunits in binding buffer at a 1:1 molar ratio. This reaction mixture was then centrifuged through a sucrose density gradient. Figure 14 shows comigration of the ^{14}C and 30S peaks with no residual radioactivity at the top of the gradient, indicating that most of the added IF-3 was bound to the subunits.

The effect of IF-3 on probe 1498-1506 binding was analyzed in two ways. First, a 16 fold excess of labeled probe was bound to subunits under normal binding conditions and increasing amounts of IF-3 were then added. After further incubation at 4°C for 30 minutes, bound probe was assayed by filter binding. This competition experiment resulted in a 62%

decrease in probe binding at a 2 fold excess of IF-3 (Figure 15). The sporadic nature of the initial data points may be due to errors in measuring small amounts of IF-3 since the protein readily binds reaction vessels and pipette tips (Hershey et al., 1981).

Probe binding in the presence of IF-3 was also analyzed by addition of IF-3 to standard filter binding assay reactions. A 1.5 fold excess of IF-3 was preincubated with subunits for 15 minutes at 37°C. Increasing amounts of labeled probe were than added and the reactions incubated on ice for a further 30 minutes. IF-3 was included in the control reactions so that any retained counts

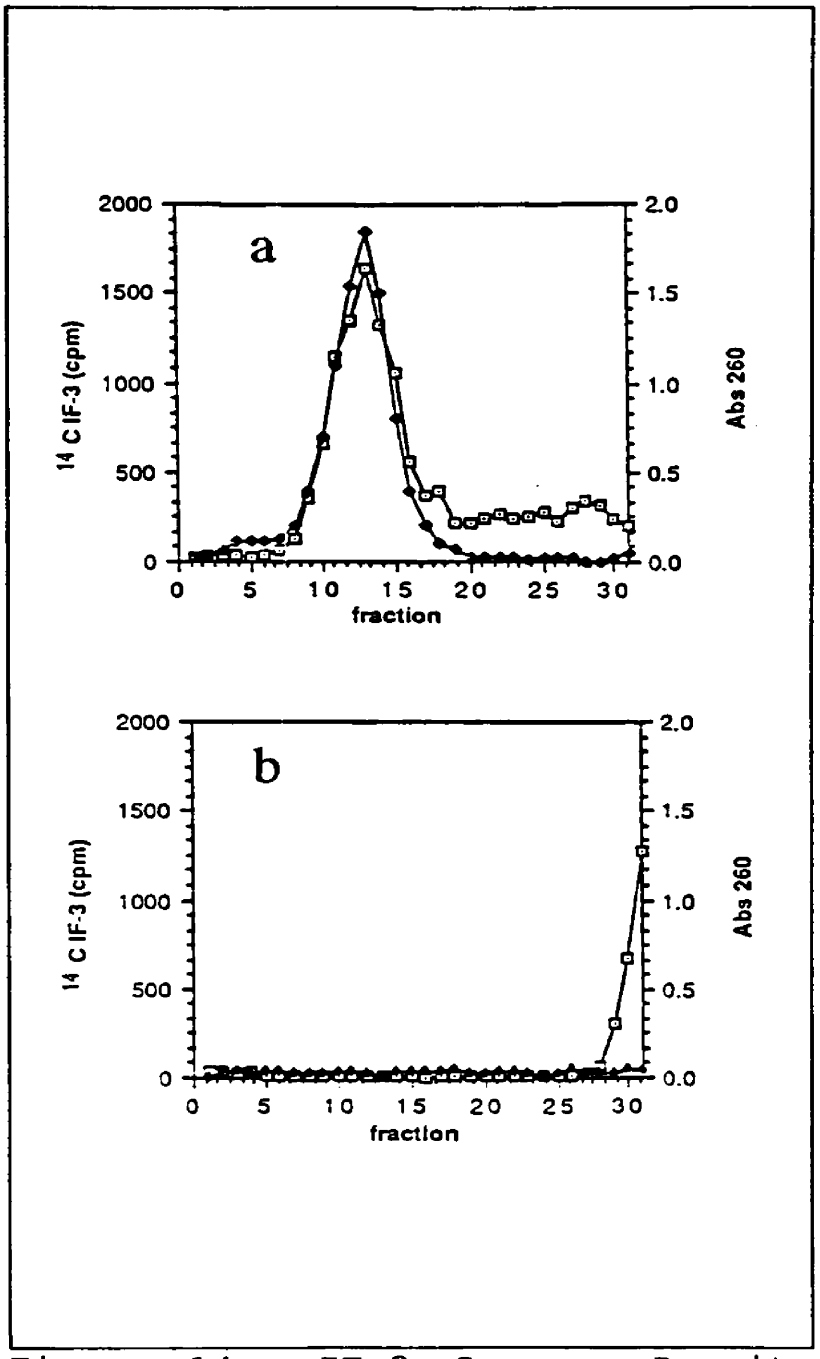

Figure 14 IF-3 Sucrose Density Gradient Binding Assay to 30S Subunits. a-equimolar amounts of ^{14}C-IF-3 and 30S subunits. b-control gradient without subunits. open squares-CPM. diamonds-absorbance (260nm).

due to non-specific probe interaction with IF-3 was subtracted. The filter binding curves in Figure 16 show an 84% decrease in probe 1498-1506 binding when IF-3 was prebound to subunits. To establish that this decrease is due to a specific interaction of IF-3 with 30S particles and not due to simply the addition of a basic protein, a mock reaction set was carried out with the protein α-chymotrypsinogen A, chosen because it is a basic protein with a molecular weight close to that of IF-3. Although binding of the oligomer was slightly reduced in the presence of α-chymotrypsinogen A, in relation to binding in the presence of IF-3 an 80% decrease was still evident.

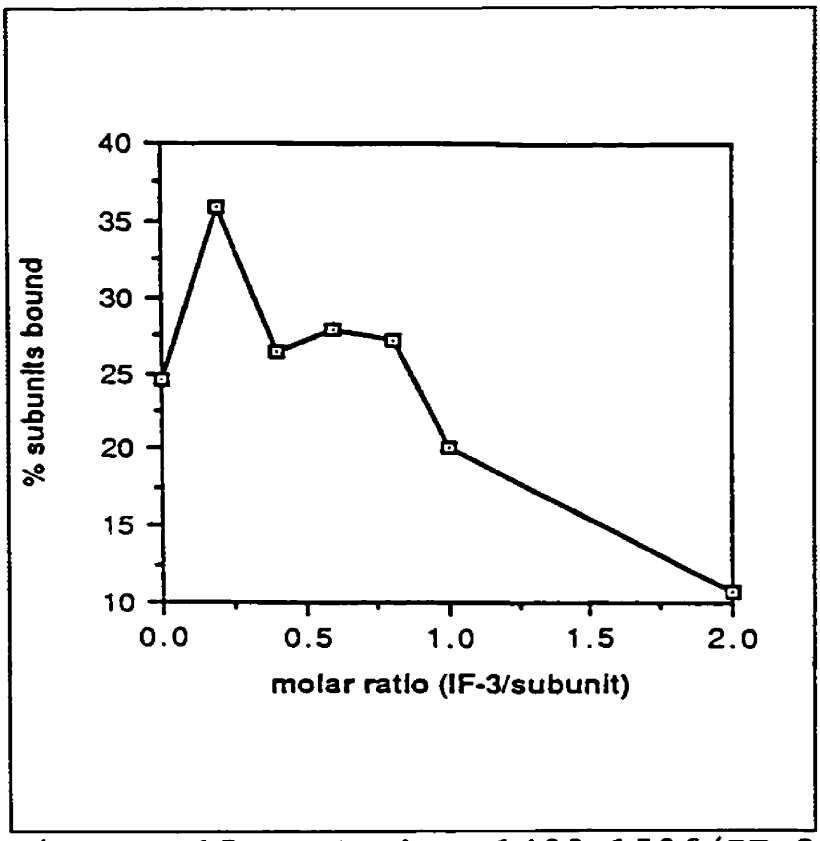

Figure 15 Probe 1498-1506/IF-3 Competition Assay. Each reaction contains a 16 fold excess of probe.

Another activity identified with IF-3 is subunit anti-association. To investigate if the apparent interaction of IF-3 at the 1500 conserved region is related to this activity, two subunit association experiments were carried out. To determine if IF-3 would indeed inhibit subunit reassociation

under the conditions of the subunit association assay, 30S subunits were preincubated with IF-3 before addition to the 50S subunits in association buffer. The gradient profile of this reaction compared to a control reaction without IF-3 (Figure 17a) indicates that the IF-3 did increase the amount of free subunits. The experiment was then repeated with probe 1498-1506 instead of IF-3 (Figure 17b). The profile shows no indication of subunit anti-association by addition of probe and implies that either the anti-association activity of IF-3 is not the result of interaction with the 1500 conserved region or that subunit association completely displaces bound probe.

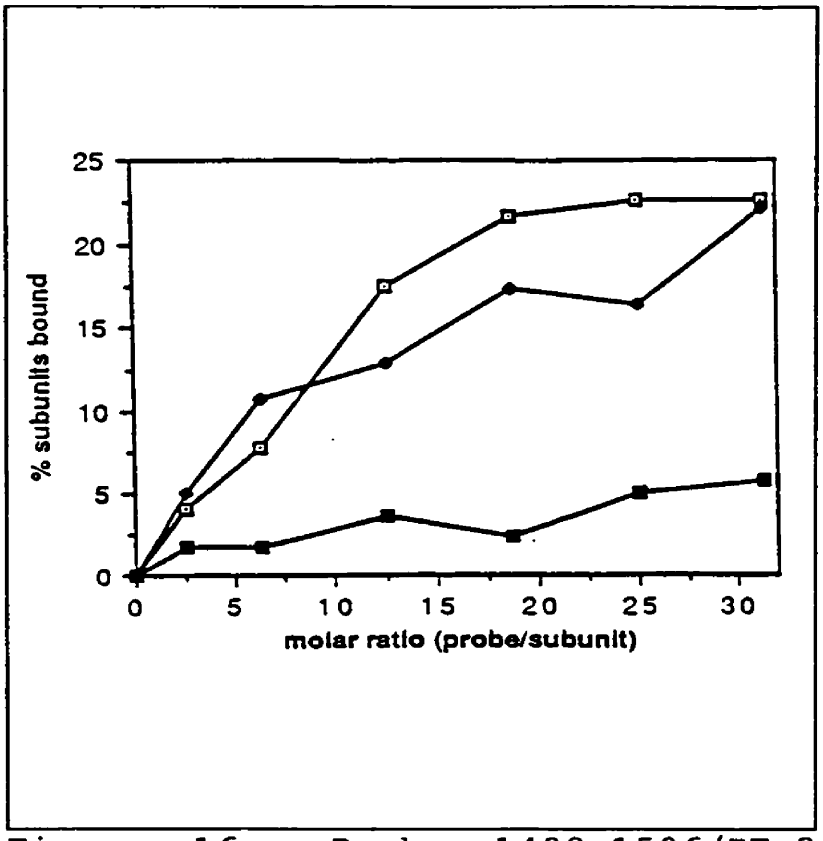

Figure 16 Probe 1498-1506/IF-3 Filter Binding Assay. open squares-control. closed squares-with IF-3. diamonds-with α-chymotrypsinogen A.

Disruption of subunit association has been demonstrated by complementary oligonucleotide binding to the 790 loop of 16S rRNA (Tapprich and Hill, 1986). To see if IF-3 interacts with this region, a competition assay was carried out as described above except probe 787-795 (see Figure 2) was

substituted for probe 1498-1506. As can be seen in Figure 18, binding of probe 787-795 was decreased by addition of IF-3 to a baseline level at about 2 fold excess of IF-3. Although this experiment was only done once and must be considered preliminary, it seems likely that the subunit anti-association activity of IF-3 effects the 790 loop.

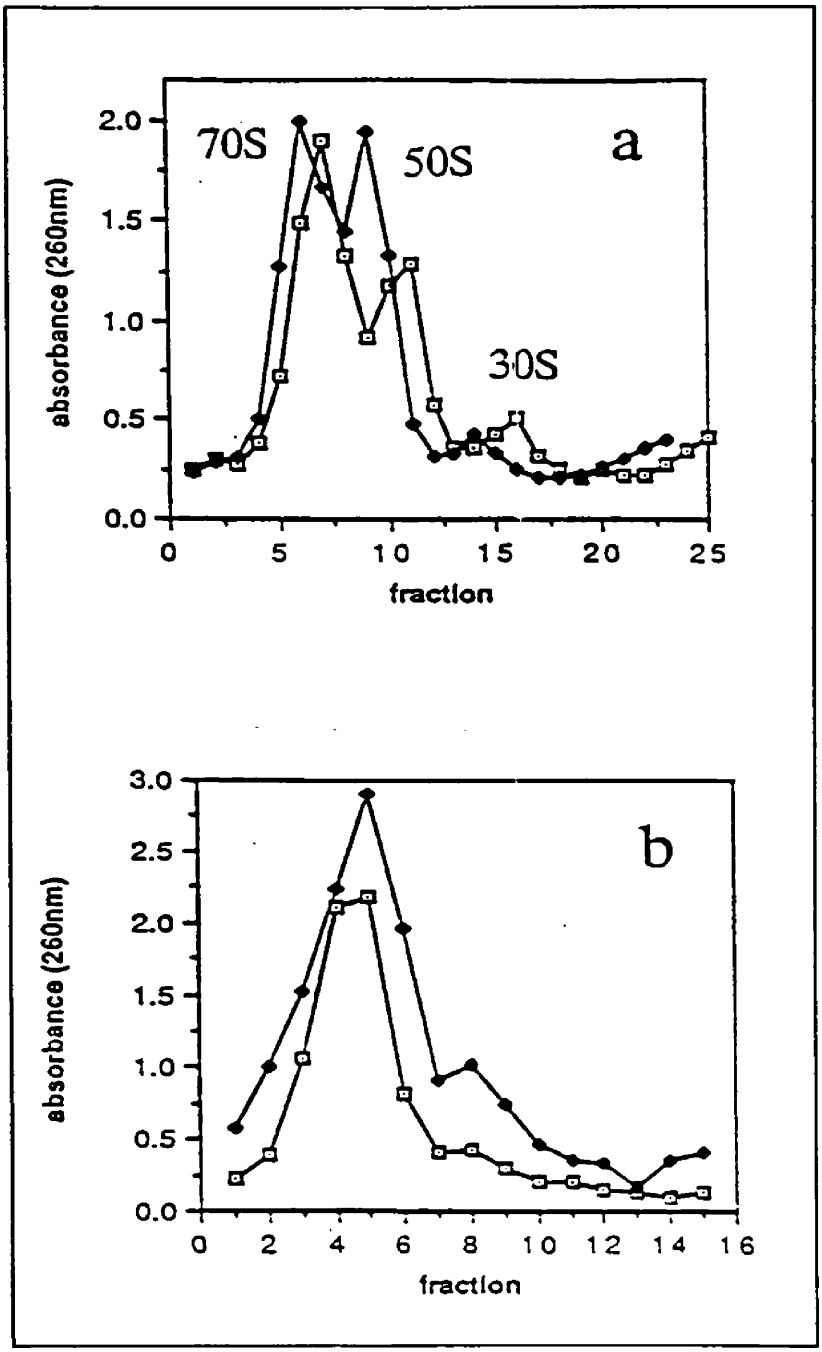

Figure 17 Subunit Association Assays. a. squares-control, diamonds-with IF-3. b. squares-control, diamonds-with probe 1498-1506.

The differential probe binding between functional states may indicate interactions between subunits and factors that inhibit the accessibility of the probe target sites. To ascertain if these differences were due to gross structural changes of the subunit when probe is bound, quasi-elastic light scattering experiments were done.

Comparison of diffusion coefficients in the presence and absence of bound 1498–1506 showed no change, suggesting that the probe did not unfold or tighten subunit structure.

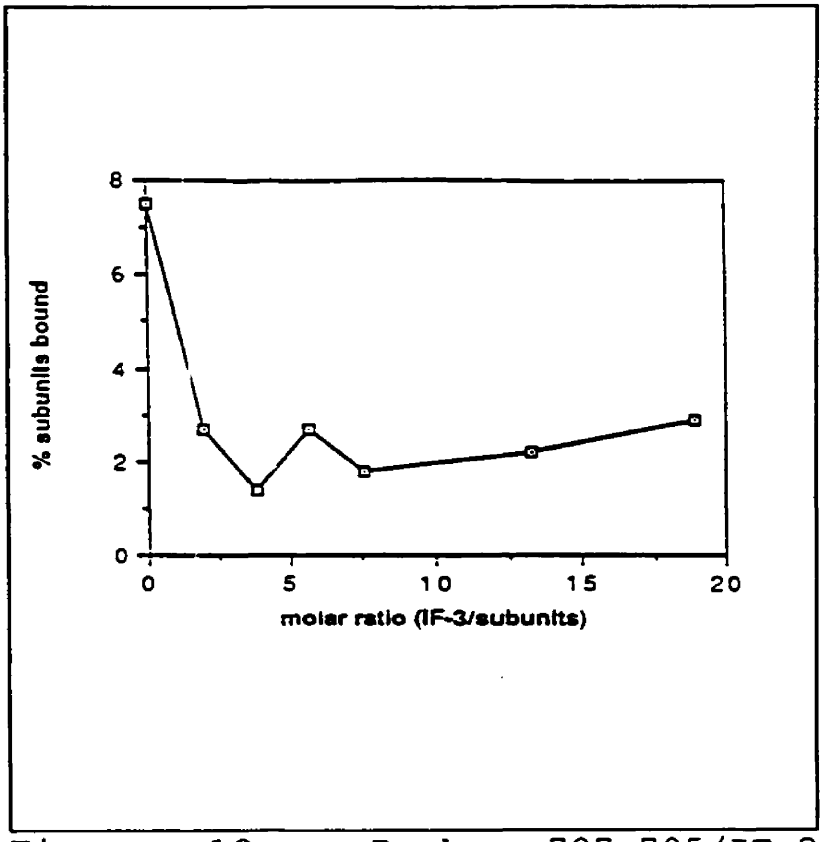

Figure 18 Probe 787–795/IF–3 Competition Assay. Increasing amounts of IF–3 were added to reactions containing 30S subunits pre–bound with probe 787–795

Chapter 4

DISCUSSION

Our current understanding of the E. coli ribosome suggests that the region downstream from the ultimate loop of 16S rRNA be exposed to the cellular milieu. It is apparent from this study that the single strand conserved region just upstream from this loop is also exposed in salt-washed free subunits and is available for interaction with translational factors. Complementary oligonucleotide probing has proven fruitful in delineating these interactions.

Central to the technique of oligomer probing is the filter binding assay which is not only used to determine target site accessibility, but also to determine differential binding between functional states. Efforts to understand characteristics of probe binding have focused on saturation levels and molar ratios of filter binding studies. A significant portion of this research project dealt with maximization of hybridization parameters and is therefore worthy of discussion.

By definition, the probe to subunit molar ratio needed to reach saturation is a function of the dissociation constant which, for small oligonucleotides, is unfortunately quite high. Another factor that may affect molar ratios is probe purity. Several times during the course of this investigation, probe preparations were encountered that showed identical binding kinetics as a normal probe sample except

that they reached saturation at uncharacteristically high molar ratios. This suggests that a portion of the probes were not participating in the hybridization reaction. Probes with incomplete removal of blocking groups, ring opening, modification of functional groups or loss of bases would be rendered less able to hybridize and thereby decrease effective probe concentration.

Saturation of filter binding curves indicates that all available subunits with accessible target sites are bound by probe. Determination as to why saturation levels are less than 100% of added subunits bound by probe was one goal of this research project. Low saturation levels indicates that some of the added subunits are unavailable for probe binding or undetected in the assay system. Indeed, examination of retention of 30S subunits indicated approximatly 50% of the subunits added were being washed through the filters under the assay conditions used for this study (data not shown). Attempts to increase subunit retention succeeded only in masking any specific binding by increasing background retention of probe.

A critical factor that may effect the availability of probe binding sites is the integrity of the subunits and rRNA. During preliminary stages of this investigation, it was found that only subunits that had been isolated under high salt conditions would yield RNase H cleavage bands. It is likely that washing away loosly bound factors and r-proteins with the

salt-wash step makes the probe target site more accessible. However, if the removal of proteins is incomplete, not all the added subunits would have available probe binding sites and, therefore, would give low saturation curves.

The integrity of the rRNA can be visualized by gel electrophoresis. It is evident in the various RNA gels presented that even subunits that migrate as a single peak in analytical ultracentrifugation runs show a certain amount of rRNA degradation. This may be due to degradation in the cell before isolation or to manipulations during isolation. Furthermore, instances of subunit unfolding may be evident in RNase H assays. Figure 7 depicts the RNase H assay used to determine the amount of time required for complete digestion of the probe/rRNA duplex. The RNase H fragment corresponding to cleavage at the probe 1492-1506 target site did not increase in intensity after 24 hours. After 48 hours, a secondary site appears to be completely clipped. The difference in cleavage between these sites may reflect the 15 base homology at the target site versus a 6 base homology at the secondary site. However, it is also possible that target site cleavage unfolds the subunit such that the secondary site becomes more available for probe binding. Since the secondary cleavage was detected only after the target site cleavage was complete the latter case seems more likely.

The change in target site accessibility upon subunit unfolding is evident in the RNase H assay in Figure 10. Here,

subunit unfolding induced by ion depletion left the target site unavailable for digestion while the secondary site was highly accessible. Thus, maintainance of a native subunit structure is required for the 1500 region to be available to probe binding.

Another factor that may have contributed to the lower than expected saturation levels is endogenous nuclease activity. In previous studies using oligomer probing of ribosomal subunits, an endogenous RNase H activity associated with isolated subunits was noted (Tapprich and Hill, 1986). Although such an activity was not seen in controls reactions of RNase H gels of this study, it is possible that residual RNase H activity could have reduced the apparent saturation of filter binding assays by removing potential probe binding sites. Aternatively, any residual endogenous DNase activity would also reduce apparent binding by removing some of added probes.

However, the relatively low saturation levels encountered do not deter the major purpose of this investigation. Information about factor interactions with the 3′ domain relies on differential probe binding between functional states. Therefore, it is not important to have 100% binding or to quantify the subunits available. It is important, however, that assay conditions maintain the native ribosomal conformation. The fact that 30S subunits used in this study migrate as a single, well defined peak in analytical

ultracentrifugation experiments indicates that hybridization conditions do not cause unfolding. Furthermore, quasi-elastic light scattering results show that probe binding does not cause gross conformational changes in subunit structure.

The major goal of this research project was to investigate the function of the conserved region of E. coli 16S rRNA between bases 1492-1506 using compementary oligonucleotides as site-specific probes. Hybridization of probes to isolated 30S subunits show that the conserved region is available for binding in the inactive form, but less available in the active form and when messenger RNA or IF-3 is bound.

Differential probe binding between functional states can be defined by two extremes. Decreases in probe binding may be due to direct competition between probe and factor for the target site. On the other hand, factor binding may cause a conformational change in the subunit that makes the target site unavailable for probe binding. Although the technique of cDNA probing cannot directly distinguish the two possibilities, the combination of probing data with information from other investigations yields a better understanding of factor interaction.

Although reduction in accessibility by some other kind of conformational change can not be ruled out, the difference in probe binding between the active and inactive forms may best be explained by the formation of pairs between bases 1394-1395

and 1505–1506 upon activation. This pairing is convincingly supported by chemical modification data (Moazed et al., 1986b) and comparative sequence analysis (Noller et al., 1986). Such an interaction suggests that the reduction in probe 1498–1506 binding upon activation is a result of direct target site competition since two of the nine possible base pairs are removed. A difference of only 40% between binding to the two structural states indicates that target site accessibility is only partially reduced. The reduction in the binding of the larger probe to the 30S subunit in the active form is much smaller. This also supports the existance of the 1394–1395/1505–1506 active base-pairing since the 15 base probe is more stably bound than the 9 base probe.

An alternative explanation for the active/inactive binding data is that the act of heating the subunits causes secondary or tertiary interactions between the probe target site and other regions of the rRNA or with ribosomal proteins. However, when filter binding assay reactions containing 1498–1506 and inactive 30S subunits were heated, the resulting binding curves were the same as unheated assays (Figure 12). This may imply that the only interaction available to decrease probe binding to active subunits is the formation of base-pairs 1394–1395/1505–1506 (the active form). On the other hand, when filter binding assay reactions were heated with 1492–1506, an enhancement of 15–mer binding was seen Figure 12), indicating that heating may transiently disrupt a

secondary or tertiary interaction and allowed a greater target site availability for probe binding.

A possible candidate for an interaction within these bases is the putative pairing between bases 1404-1405 and 1496-1497. This pairing is well supported by comparative sequence analysis (Noller et al., 1986) as well as nuclease digestion (Douthwaite et al., 1983) and chemical modification (Noller, 1974; Moazed et al., 1986a) at low temperatures, but is not found at 37°C. Therefore, the increase in 1492-1506 binding in the heated filter binding assays is probably due to the disruption of base pairs between 1404-1405/1496-1497 at the higher temperature. The pairing of bases 1404-1405/1496-1497 is central to the induced coaxial stacking model for tRNA binding (Noller et al., 1986) (Figure 1).

Whereas a reduction of 40% is seen for binding of probe 1498-1506 to 30S subunits in the active state, reduction in the presence of poly U is much more dramatic (Figure 13). The reduction from 23% added subunits bound without poly U to about 7% with poly U represents a 70% change in binding and is apparently independent of activation state. Direct competition of poly U and the probe for target site binding is one explanation for this reduction, however, a model in which poly U not only partially blocks the target site, but also changes the conformation of the region is possible. Such a conformational change upon poly U binding is supported by evidence that addition of polynucleotides to the subunits

under reactivation conditions greatly enhances the rate of active subunit formation (Zamir et al., 1974).

Poly U directed $tRNA^{Phe}$ binding had little effect on probe target site accessibility. Although probe binding with tRNA present was consistently slightly lower than with poly U alone, the significance of this decrease is questionable. Interaction of the $tRNA^{Phe}$ anticodon around bases 1399–1401 has been convincingly demonstrated (Ofengand et al., 1979; Prince et al., 1982; Meier and Wagner, 1984; Moazed and Noller, 1986). As with the case of the active base-pairs, it is probable that poly U masks any effect due to tRNA binding.

A picture of the interactions of the 1500 conserved region emerges from the discussion above. Data from this study show that the target site for probe 1498–1506 and probe 1492–1506 is available for binding in the inactive subunit, but is less available upon activation. This supports the formation of the active base-pairs which requires the juxtaposition of the 1500 region with the 1400 region. The binding characteristics of the two probes are also consistant with the interaction of bases 1404–1405/1496–1497. Whereas activation only partially attenuates probe binding, poly U produces a much greater exclusion suggesting that poly U blocks more of the oligomer binding site. Since mRNA and tRNA are both interacting in the same region, it is not surprising that poly U directed tRNA binding had little effect on the probe target site.

Taken together, the data of this study provide basis for a possible model of the interactions around the decoding site. The model presented in Figure 19 provides for the 3-4 fold stabilization of tRNA binding upon codon/anticodon base pairing by stacking of the P-site interaction with 1394-1395/1505-1506 and stacking of the A-site interaction with 1404-1405/1496-1497. This model is very similar to the induced coaxial stacking model presented by Noller and coworkers (Noller et al., 1986). However, the Noller model does not address the active/inactive transformation and includes only a stacking interaction with 1404-1405/1496-1497. Although the coaxial stacking model leaves open the question of which tRNA stacks, they suggest the P-site be stacked to 1404-1405/1496-1497 because under the conditions of C1400 cross-link formation, the bound tRNA is puromycin reactive. However, this argument could just as easily place the P-site stacked with 1394-1395/1505-1506 since the subunit must be in the active form for poly U directed tRNA binding. Futhermore, the placement of P- and A-sites in Figure 19 is justified by satisfying the following criterion:

(1) The A-site, by its nature, is the site of proofreading. Since antibiotics that effect proofreading bind to the penultimate helix at bases 1409-1491 (Noller et al., 1986), it seems more logical to place the A-site rather than the P-site closer to bases 1409-1491.

(2) Available evidence suggests that tRNA binding is

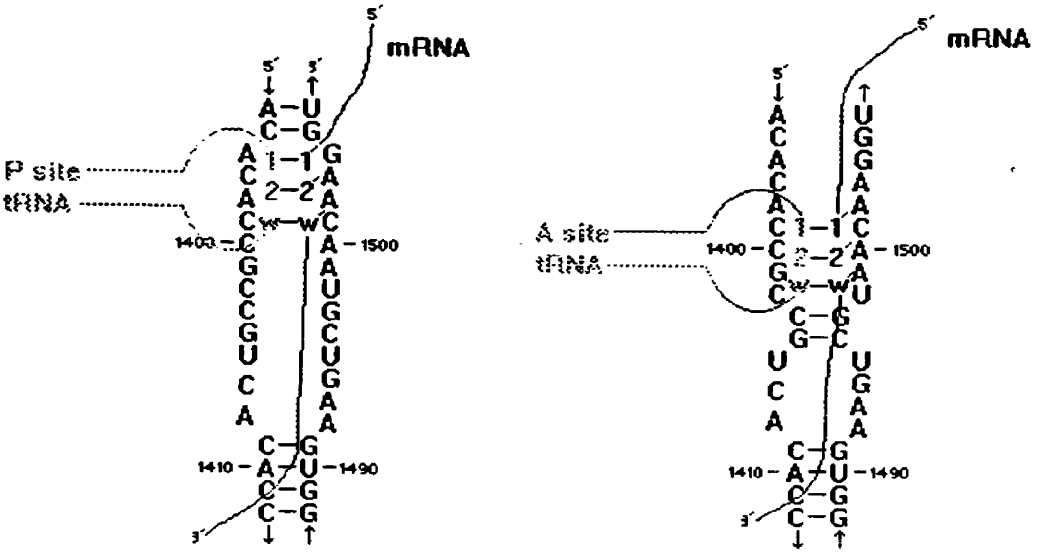

Figure 19 Proposed Model for Interactions at the 1500 Region. Diagram of the decoding site showing the relative positions of mRNA and tRNAs. The proposed alternate stacking of the P-site and A-site tRNAs are shown.

stabilized by a 5′ stack (Rich and RajBhandary, 1976) which is provided for in the model by the A-site. The Noller model indicates a 3′ stack for the P-site.

(3) Electron microscopic localization of certain features of 16S rRNA places the 1400 and 1500 regions within the cleft of the 30S subunit with the ultimate loop higher in the cleft than the penultimate loop (Noller and Woese, 1981; Brimacombe et al., 1988). Current evidence suggests that the P-site is enclosed higher in the cleft and the A-site is lower and more available for incoming tRNA. Such a situation is consistant with the geometry of the model presented in Figure 19.

(4) The model presents a geometry that accomodates the Shine-Dalgarno interaction and places a start codon in the decoding site, easily accounting for the 7-10 bases between the two (Steitz and Jakes, 1975).

(5) Although both tRNA binding sites are stabilized by stacking interactions with rRNA, the fluidity necessary for translocation may be maintained by the active/inactive switch. This suggests that the active/inactive transformation is a process inherent in the protein biosynthesis apparatus and not an artifact of isolation.

(6) Finally, the model accounts for the inability of $tRNA^{Phe}$ to bind inactive subunits since the stabilization by stacking to base-pairs 1394-1395/1505-1506 is not possible.

Studies of ribosomal RNA structure and function using

poly U must be carefully interpreted. Since it lacks a Shine-Dalgarno region and a start codon, poly U directed translation may be considered artifactual. However, poly U can direct synthesis of polyphenylalanine and therefore may represent translation during elongation. Extrapolation to the initiation state can only be done in the sense of general geometry.

The attenuation of probe 1498-1506 binding in the presence of IF-3 (Figure 15) suggests that the 1500 conserved region plays a role in initiation. It is unclear whether IF-3 reduces probe binding by directly binding the target site or by forcing the region into a conformation unfavorable to probe access on the intact 30S subunit. It is clear that IF-3 directly binds to the 49 base colicin fragment (bases 1493-1542) in solution (Wickstrom, 1983) since IF-3 enhanced and protected bases in nearly alternating fashion from base 1494-1530. This pattern was relatively insensitive to increasing salt concentration, suggesting the factor interacts directly and not electrostatically. The direct binding to this region is further supported by a cross-link between IF-3 and bases 1506-1529 _in situ_ (Ehresmann _et al._, 1986).

Since the Wickstrom nuclease digestion study was carried out with the colicin fragment in solution, it is difficult to extrapolate to intact 30S subunits. It seems likely that IF-3 partially binds the probe target site, perhaps by binding to one side of the RNA helix. This would explain the incomplete

reduction in probe binding when more than stoichiometric amounts of IF-3 were present and the partial availability of the site to nulcease digestion on the colicin fragment.

Two functional activities have been proposed for IF-3. One deals with an interaction with the 3′ domain as indicated above. The other deals with subunit anti-association. In order to investigate this second activity, the effect of IF-3 on probe 787-795 binding was determined. Probe 787-795 was previously shown to attenuate subunit association by inhibiting base pairing with a complementary region of 23S rRNA (Tapprich and Hill, 1986). Preliminary evidence shows that 787-795 binding is indeed attenuated in the presence of IF-3 (Figure 18) suggesting that the subunit anti-association function of IF-3 is at least partially due to a change in the accessibility of the 790 loop. It is unclear whether this interaction is a direct binding of IF-3 to the 790 loop or due to a conformational change. Given the direct binding of IF-3 to the 3′ domain and the IF-3 cross-link to bases 819-859 (Ehresmann et al., 1986), it seems likely that the subunit anti-association activity is mediated by a conformational change. However, more experimental evidence is required before a definitive answer is obtained.

Recent experiments involving the interaction of IF-3 with the 3′ domain of 16S rRNA indicate that the relm of influence of IF-3 does not include the Shine-Dalgarno interaction and that the function of IF-3 does not include the direct

recognition or binding of mRNA (Canonaco et al., 1987; Gualerzi et al., 1988). Rather, IF-3 acts to stimulate the on and off rate of tRNAs during initiation until the correct initiator tRNA/start codon interaction occurs (Gualerzi et al., 1988). In light of the probe binding evidence presented in this study indicating that IF-3 and mRNA interact with the same region of rRNA (within bases 1498-1506), it is possible that this IF-3 proofreading function is accomplished by disruption of the decoding site such that the major interaction of initiator tRNA with the 30S subunit is via basepairing with the start codon. In other words, IF-3 minimizes any stabilization of tRNA binding due to interaction with 30S subunits and maximizes the codon/anticodon interaction. It is interesting to think that this disruption includes the breaking of the active base-pairs and thereby removing the stacking stabilization of tRNA.

From the data and discussion above, an intriging possible picture of the decoding site during initiation and elongation emerges. During formation of the initiation complex, IF-3 binds and destabilizes the ultimate helix. The associated conformational change opens the decoding site allowing a rapid exchange of incoming tRNA. Upon formation of the 70S initiation complex, IF-3 dissociates and the codon/anticodon interaction is stabilized by the newly formed active base-pairs. At this point, the stacking base-pairs are not yet formed, allowing better access of the incoming aminoacylated-

tRNA to the next codon, but as the correct codon/anticodon interaction is formed, the stacking base-pairs form and thus stabilizes the A-site tRNA. In concert with the formation of the stacking pairs, the active base-pairing disrupts, making way for the movement of the P-site tRNA to the exit site after peptidyl transfer. This cycle of breaking and forming stacking pairs allows for the fluidity necessary to the movement of the tRNAs and mRNA during protein synthesis, but also allows for stabilization of the correct codon/anticodon pairing. Thus, the model presented in Figure 19 represents a transition state rather than a discrete intermediate.

The model of the decoding site as presented in Figure 19 has eight bases between stacking base-pairs in the 1400 region and only seven bases in the 1500 region. The extra base in the 1400 region may act as a fulcrum during stacking transitions. Furthermore, the eighth base may account for the "kink" between codons (Rich,1974; Fuller and Hodgson, 1967; Sundaralingam et al.,1975; Pongs, 1978) necessary to accomodate the tRNA bulk upon close approach at the anticodons.

This model of the interactions at the decoding site is speculative at this point, but does provide a framework for further experimentation. Several experiments using cDNA probes come to mind that may better define the fine structure of the region. Using a probe to bases 1496-1504 and another to bases 1498-1504 under the various conditions described

above would better define the role of the stacking base-pairs. Mapping with six-base probes that span the entire 1500 conserved region in one base increments would also prove enlightening. Further investigation into the role of IF-3 in the region could be accomplished by using a probe to destabilize the ultimate helix and perhaps mimic IF-3 binding.

In summary, the research discussed provides a better understanding of the interactions at the 1500 conserved region of 16S rRNA. Specifically, it was found that the target site was available for probe bindng in the inactive salt-washed subunit, but was attenuated by activation, IF-3 bindng and to a greater extent by poly U binding. Using these data and other available information, a model was presented that may explain the role of rRNA at the decoding site. Finally, this project provided insight into the mechanics and value of the cDNA probing technique as a tool for investigating the structure and function of ribosomal RNA.

REFERENCES

Benne, R., M. Brown-Luedi and J. Hershey In K. Moldave (ed.): RNA and Protein Synthesis. New York: Academic Press, pp.309-329.

Blair, D., L. Heilmann and W. Hill (1981) Biophys. Chem. 14: 81-89.

Bloomfield, V. (1981) Ann. Rev. Biophysics Bioeng. 10: 421-458.

Boublik, M., G. Oostergetel, J. Wall, J. Hainfeld, M. Radermacher, T. Wagenknecht, A. Verschoor and J. Frank (1986) In B. Hardesty and G. Kramer (eds.): Structure, Function, and Genetics of Ribosomes. New York: Springer-Verlag, pp. 68-86.

Brimacombe, R., and W. Steige (1985) Biochem. J. 229: 1-17.

Brimacombe, R., J. Atmadja, A. Kyriatsoulis, and W. Stiege (1986) In B. Hardesty and G. Kramer (eds.): Structure, Function, and Genetics of Ribosomes. New York: Springer-Verlag, pp. 184-202.

Brimacombe, R., J. Atmadja, W. Stiege and D. Schuler (1988) J. Mol. Biol. 199: 115-136.

Canonaco, M., C. Pon, R. Pawlik, R. Calogero and C. Gualerzi (1987) Biochimie 69: 957-963.

Cantor, C. and K. Huang (1975) J. Mol. Biol. 47: .

Carbon, P., C. Ehresmann, B. Ehresmann and J.-P. Ebel (1978) FEBS Lett. 94: 152-156.

Capel, M., D. Engelman, B. Freeborn, M. Kjeldgaard, J. Langer, V. Ramakrishnan, D. Schindler, D. Schneider, B. Schoenborn, I.-Y. Sillers, S. Yabuki and P. Moore (1987) Science 238: 1403-1406.

Cech, T. (1986) Cell 44: 207-210.

Dahlberg, A. (1989) Cell 57: 525-529.

Dams, E., L. Hendriks, Y. Van de Peer, J.-M. Neefs, G. Smits, I. Vandenbempt and R. De Wachter (1988) Nucl. Acids Res. 16:r87-r173.

Donis-Keller, H., A. Maxam and W. Gilbert (1977) Nucl. Acids Res. 4: 2527-2537.

Douthwaite, S., A. Christensen and R. Garrett (1983) J. Mol. Biol. 169: 249-279.

Ehresmann, C., H. Moine, M. Mougel, J. Dondon, M. Grunberg-Manago, J.-P. Ebel and B. Ehresmann (1986) Nucl. Acids Res. 14: 4803-4821.

Erdmann, V., T. Pieler, J. Wolters, M. Digweed, D. Vogel, and R. Hartmann (1986) In B. Hardesty and G. Kramer (eds.): Structure, Function, and Genetics of Ribosomes. New York: Springer-Verlag, pp. 164-183.

Fuller, W., and A. Hodgson (1967) Nature 215: 817-821.

Gualerzi, C., R. Calogero, M. Canonaco, M. Brombach and C. Pon (1988) In M. Tuite, M Picard and M. Bolotin-Fukuhara (eds.): Genetics of Translation. Berlin: Springer-Verlag, pp. 317-330.

Ginzburg, I., R. Miskin and A. Zamir (1973) J. Mol. Biol. 79: 481-494.

Giri, L., W. Hill and H. Wittmann (1984) In C. Anfinsen, J. Edsall and F. Richards (eds.): Advances in Protein Chemistry. New York: Academic Press, pp. 1-78.

Gutell, R., B. Weiser, C. Woese and H. Noller (1985) Prog. Nucl. Acids Res. Mol. Biol. 32: 156-216.

Hardesty, B., O. Odem and H.-Y. Deng (1986) In B. Hardesty and G. Kramer (eds.): Structure, Function, and Genetics of Ribosomes. New York: Springer-Verlag, pp. 495-508.

Hill, W., G. Rossetti and K. Van Holde (1969) J. Mol. Biol. 44: 263-277.

Hill, W., J. Thompson and J. Anderegg (1969) J. Mol. Biol. 44: 89-99.

Hill, W. and A. Tassanakajohn (1987) Biochimie 69: 1071-1080.

Keren-Zur M., M. Boublik and J. Ofengand (1979) PNAS 76: 1054-1058.

Lake, J. (1980) In G. Chambliss, G. Craven, J. Davies and K. Davis (eds.): Ribosomes: Structure, Function and Genetics. Baltimore: University Park Press, pp. 207-236.

Lake, J. and L. Kahan (1975) J. Mol. Biol. 99: 631-644.

Maxam, A. and W. Gilbert (1980) Methods Enzymol. 65: 499-559.

Meier, N. and R. Wagner (1984) Nucl. Acids Res. 12: 1473-1487.

Moazed, D. and H. Noller (1986) Cell 47: 973-984.

Moazed, D., S. Stern and H. Noller (1986a) J. Mol. Biol. 187: 399-416.

Moazed, D., B. Van Stolk, S. Douthwaite and H. Noller (1986b) J. Mol. Biol. 191: 483-493.

Moore, P., M. Capel, M. Kjeldgaard and D. Engelman (1986) In B. Hardesty and G. Kramer (eds.): Structure, Function, and Genetics of Ribosomes. New York: Springer-Verlag, pp. 87-100.

Noller, H. (1974) Biochem. 13: 4694-4703.

Noller, H. (1980) In G. Chambliss, G. Craven, J. Davies and K. Davis (eds.): Ribosomes: Structure, Function and Genetics. Baltimore: University Park Press, pp. 3-49.

Noller, H. and C. Woese (1981) Science 212: 403-411.

Noller, H. (1984) Annu. Rev. Biochem. 53: 119-192.

Noller, H., M. Asire, A. Barta, S. Douthwaite, T. Goldstein, R. Gutell, D. Moazed, J. Normanly, J. Prince, S. Stern, K. Triman, S. Turner, B. Van Stolk, V. Wheaton, B. Weiser and C. Woese (1986) In B. Hardesty and G. Kramer (eds.): Structure, Function, and Genetics of Ribosomes. New York: Springer-Verlag, pp. 143-163.

Nomura, M. and W. Held (1974) In M. Nomura, A. Tissieres and P. Lengyel (eds.): Ribosomes. Cold Spring Harbor Laboratory, pp. 193-223.

Oakes, M., M. Clark, E. Henderson and J. Lake (1986) PNAS 83: 275-279.

Ofengand, J., R. Liou, J. Kohut, I. Schwartz and R. Zimmermann (1979) Biochem. 18: 4322-4332.

Ofengand, J., P. Gornicki, K. Chakraburtty and K. Nurse (1982) PNAS 79: 2817-2821.

Pongs, O. (1978) In S. Altman (ed.): Transfer RNA. Cambridg, Massachusetts, M.I.T. Press. pp. 78-104.

Prince, J., B. Taylor, D. Thurlow, J. Ofengand and R. Zimmerman (1982) PNAS 79: 5450-5454.

Rich, A. (1974) In M. Nomura, A. Tissieres and P. Lengyel (eds.): Ribosomes. Cold Spring Harbor Laboratory, pp. 871-884.

Rich, A. and U. RajBhandary (1976) Ann. Rev. Biochem. 45: 805-860.

Schleich, T., E. Wickstrom, K. Twombly, B. Schmidt and R. Tyson (1980) Biochem. 19: 1651-1656.

Schwartz, I. and J. Ofengand (1978) Biochem. 45: 805-860.

Shine, J. and L. Dalgarno (1974) PNAS 71: 1342-1346.

Sharp, P. (1987) Cell 50: 147-148.

Spirin, A. (1986) Ribosome Structure and Protein Biosynthesis. Menlo Park: Benjamin/Cummings. pp.62-68.

Spitnik-Elson, P., D. Elson, S. Avital and R. Abromowitz (1985) Nucl. Acids Res. 13: 4719-4738.

Stark, B., R. Kole, E. Bowman and S. Altman (1978) PNAS 75: 3717-3721.

Steitz, J. and K. Jakes (1975) PNAS 72: 4734-4738.

Stern, S., B. Weiser and H. Noller (1988) J. Mol. Biol. 204: 447.

Stern, S., T. Powers, L.-M. Changchien and H. Noller (1989) Science 244: 783-790.

Stöffler, G. and M. Stöffler-Meilicke (1981) In Schweiger, H. (ed.): International Cell Biology. Heidelberg: Springer-Verlag, pp. 93-102.

Stöffler, G. and M. Stöffler-Meilicke (1984) Ann. Rev. Biophys. Bioeng. 13: 409-455.

Stöffler, G. and M. Stöffler-Meilicke (1986) In B. Hardesty and G. Kramer (eds.): Structure, Function, and Genetics of Ribosomes. New York: Springer-Verlag, pp. 28-46.

Sundaralingam, M., T. Brennan, N. Yathindra and T. Ichikawa (1975) In M. Sundaralingam and S. Roa (eds.): Structure and Conformation of Nucleic Acids and Protein-Nucleic Acid Interactions. Baltimore, Maryland: University Park Press, pp. 101-115.

Tam, M. and W. Hill (1981) Biochem. 20: 6480-6484.

Tapprich, W. and W. Hill (1986) PNAS 83: 556-560.

Traut, R., J. Lambert, G. Boileau and J. Kenney (1980) In G. Chambliss, G. Craven, J. Davies, K. Davis, L. Kahan and M.

Nomura (eds.): Ribosomes: Structure, Function and Genetics. Baltimore: University Park Press, pp. 89–110.

Trifonov, E. (1987) J. Mol. Biol. 194: 643–652.

Van Holde, K. and W. Hill (1974) In M. Nomura, A. Tissieres and P. Lengyel (eds.): Ribosomes. Cold Spring Harbor Laboratory, pp.53–91.

Vasiliev, V., I. Serdyuk, A. Gudkov and A. Spirin (1986) In B. Hardesty and G. Kramer (eds.): Structure, Function, and Genetics of Ribosomes. New York: Springer–Verlag, pp. 128–142.

Vogel Z., T. Vogel, A. Zamir and D. Elson (1970) J. Mol. Biol. 54: 379–386.

Wickstrom, E. (1983) Nucl. Acids Res. 11: 2035–2052.

Wittmann, H., (1983) Ann. Rev. Biochem. 52: 35–65.

Wittmann, H., (1986) In B. Hardesty and G. Kramer (eds.): Structure, Function, and Genetics of Ribosomes. New York: Springer–Verlag, pp. 1–27.

Zamir, A., R. Miskin and D. Elson (1969) FEBS Lett. 3: 85–88.

Zamir, A., R. Miskin and D. Elson (1971) J. Mol. Biol. 60: 347–364.

Zamir, A., R. Miskin, Z. Vogel and D. Elson (1974) Methods Enzymol. 30: 406–426.

Zimmermann, R. (1980) In G. Chambliss, G. Craven, J. Davies, K. Davis, L. Kahan and M. Nomura (eds.): Ribosomes: Structure, Function and Genetics. Baltimore: University Park Press, pp. 135–169.